6-2019

Chronostratigraphic Correlation of the Burnt Bluff Group across the Michigan Basin, USA

Mohammed A. Al-Musawi

CHRONOSTRATIGRAPHIC CORRELATION OF THE BURNT BLUFF GROUP ACROSS THE MICHIGAN BASIN, USA

by

Mohammed A. Al-Musawi

A thesis submitted to the Graduate C college
in partial fulfillment of the requirements
for the degree of Master of Science
Geosciences
Western Michigan University
June 2019

Thesis Committee:

Stephen Kaczmarek, Ph.D.
William Harrison III, Ph.D.
Peter Voice, Ph.D.

ACKNOWLEDGMENTS

I would like to thank my wife, Elaf, for her unconditional faith, support, and patience as I have worked on this thesis. My parents, Ahmed and Assma Al-Musawi, for the enormous sacrifices they did to make my life better. My best friend, Zaid Nadhim, who has been there every day by my side. My advisor, Steve Kaczmarek, for his tremendous support, trust, and for teaching me how to be a good thinker. My committee members, Bill Harrison and Peter Voice for their support and vast knowledge. Dr. Jeffery Kuglitsch for all the time and energy he put into dissolving rock and picking conodonts for this study. A personal thank you to Linda Harrison, John Yellich, and Jennifer Trout for making MGRRE a second home for me over the past 3 years. Thank you all for your support.

Mohammed Al-Musawi

CHRONOSTRATIGRAPHIC CORRELATION OF THE BURNT BLUFF GROUP ACROSS THE MICHIGAN BASIN, USA

Mohammed A. Al-Musawi, M.S.

Western Michigan University, 2019

In the Michigan Basin, the Burnt Bluff Group (BBG) is lower Middle Silurian in age (Llandovery), and is composed of limestones and dolostones. The BBG is bounded above by the Schoolcraft Formation and below by the Cabot Head Shale. The BBG in northern Lower Michigan is composed of three formations, including the Lime Island, Byron, and Hendricks, which reflect deposition on a broad shallow marine shelf. In contrast, the BBG in central Michigan is composed of a single lithologic unit called informally the "undifferentiated BBG (UD-BBG)," which reflects deposition in a deeper marine basin. Lithostratigraphically, the three formations in the north have been historically correlated to the UD-BBG in the south. The above lithostratigraphic model was evaluated in this study through integration of conodonts, stable carbon isotopes, and $^{87}Sr/^{86}Sr$ data, which were extracted from 5 cores in the Michigan Basin. These data were used to constrain the ages of the BBG in the Michigan Basin in order to establish a chronostratigraphic correlation from shelf to basin. In the shelf position, one positive, +4‰ VPDB, carbon isotope excursion (CIE) was identified. Conodont biostratigraphy constrains the age of this excursion to the global Late Aeronian excursion. In the slope position, which lies between the shelf and basin-center, three positive excursions (2.2-2.5‰, 5‰, +3‰ VPDB) were identified. Conodont age dates and $^{87}Sr/^{86}Sr$ data constrain these three positive excursions to the global Early Aeronian excursion, Late Aeronian excursion, and Valgu excursion, respectfully. In the basin-center position, two positive excursions were identified, +2-2.2‰, +3‰. Based on $^{87}Sr/^{86}Sr$, these excursions were identified as the global Early Aeronian excursion, and the Late Aeronian excursion, respectfully. The age-constrained CIEs were used to correlate rock units between the three positions. These correlations imply that the existing lithostratigraphic model is not accurate, and that the BBG was deposited at different times in the different locations in the basin.

Table of Contents

List of Tables

List of Figures:

Chapter 1
Introduction

1.1. Introduction

The Burnt Bluff Group (BBG) is one of several hydrocarbon-producing carbonate units in the Michigan Basin (Voice et al. 2017). According to a recent USGS assessment (USGS 2015), the BBG potentially contains 43.8 BCGF of gas and 0.8 MMBNGL of natural gas liquids. Compared to other Silurian-age hydrocarbon plays in the Michigan Basin, however, production from the BBG has been relatively modest. As such, research studies on the sedimentology, stratigraphy, and diagenesis of the BBG have been more limited in scope compared to hydrocarbon producers Silurian strata, such as the pinnacle reef complexes and the associated evaporites of the Niagaran-Lower Salina units (e.g., Harrison 1985; Sears and Lucia 1979; Friedman and Kopaska-Merkel 1991; Grammer et al. 2010; Rine et al. 2017a,b; Rine et al. in review).

The BBG is lower Middle Silurian in age (Ehlers and Kesling 1957; Kuglitsch 2000) and is composed of limestones and dolostones. Stratigraphically, the BBG bounded above by the Schoolcraft Fm. (Manistique Group) and below by the Cabot Head Shale (Cataract Group) (Fig. 1). Much of what we know about the geology of the BBG comes from outcrop and core studies. Outcrops and quarries with exposed BBG in Michigan's Upper Peninsula are distributed in an arcuate belt from the Garden Peninsula in the west to the eastern tip of the Upper Peninsula (Fig. 2) (Ehlers and Kesling 1957). These outcrops are characterized by three distinct lithostratigraphic units including the Lime Island, the Byron, and the Hendricks Formations (Ehlers 1921; Cumings and Ehlers 1942; Ehlers and Kesling 1957). Only a few studies have investigated the BBG in the subsurface in the Michigan Basin (e.g., Harrison 1985; Voice et al. 2017). Necessarily, subsurface studies focused on using Gamma Ray (GR) wire-line logs, and limited core data to make basin-wide stratigraphic correlations between wells. Because the BBG is positioned between two widespread lithologic units, the Schoolcraft and Cabot Head Shale, with distinct GR signatures it is relatively easy to identify the lower and upper contacts of the BBG. Therefore, lithostratigraphic correlation of the BBG across the basin using the GR log represents the existing model.

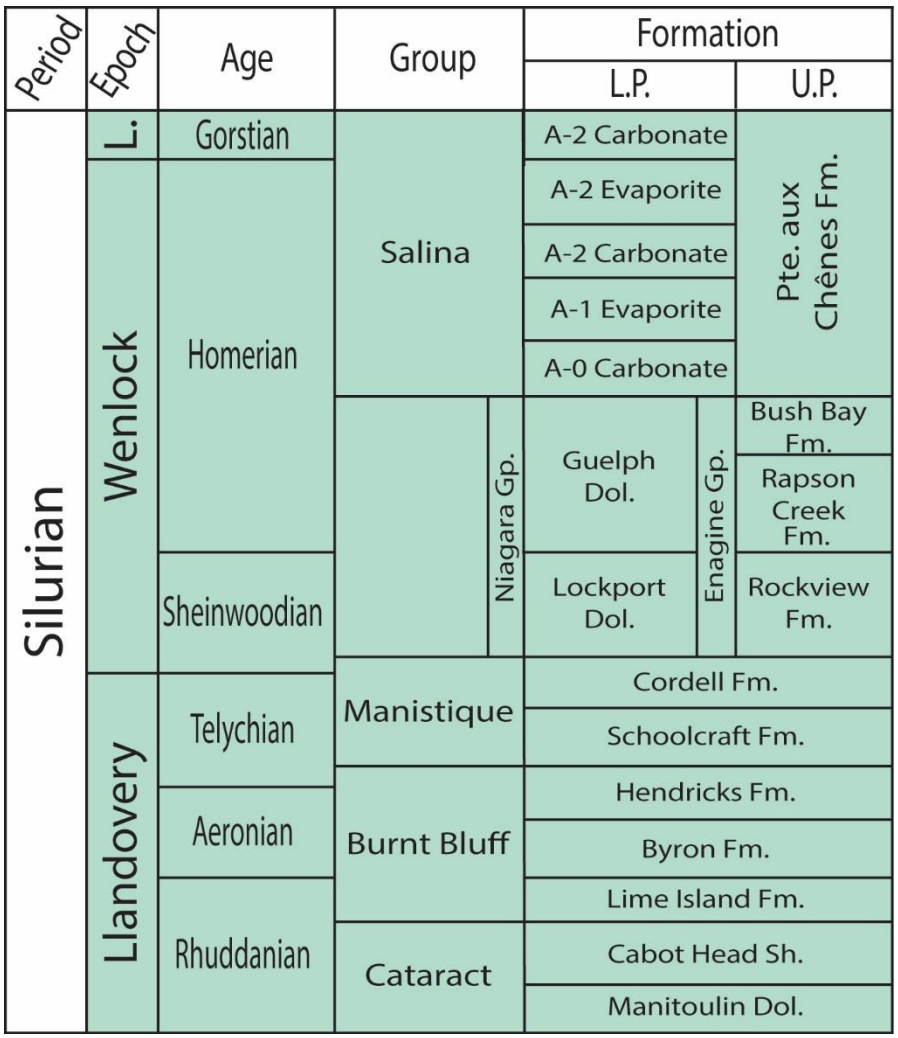

Figure 1: The Lithostratigraphic nomenclature for the Early Silurian (Llandovery) in the Michigan Basin. Modified after Voice et al. (2017).

According to the correlation by Harrison (1985), the BBG in the central basin consists of a single lithologic unit characterized by a homogeneous burrowed carbonate mudstone. Harrison (1985) referred to this unit as the "Manistique-like" facies. To avoid confusion with the overlying Manistique Group, this depositional unit will be referred to herein as the Undifferentiated BBG (UD-BBG) following the suggestion of Kuglitsch (2000). Core description work by Harrison (1985) suggests that the BBG transitions from near-shore, intertidal/supratidal and subtidal shelf and reef complex facies, which are represented by three distinguishable formations (i.e. the Lime Island, the Byron, and the Hendricks Formations) in the northern part of the Michigan Basin, to deeper open marine facies represented by only one unit (i.e. the undifferentiated BBG) in the central basin.

The overarching goal of the current study is to augment the limited chronological understanding of the BBG in the Michigan Basin by developing a basin-wide chronostratigraphic correlation by integrating multiple datasets. Including conventional wireline tools, detailed core description, biostratigraphy data (conodonts), strontium isotopes, and stable carbon isotope data. The main objectives of this study are to: (i) Constrain the age of the BBG in the Michigan Basin; and (ii) establish a chronostratigraphic correlation of the BBG from shelf to basin-center. The principal hypothesis of this study is that the BBG in northern lower Michigan, that includes Lime Island, Byron, and Hendricks Formations, is a time equivalent of the UD-BBG in central Michigan. Specifically, this study will evaluate the claim that isotopic data can be used to identify geologically relevant depositional packages in the otherwise homogeneous UD-BBG.

1.2. Geological Context

The Michigan Basin is an intra-cratonic basin that covers approximately 260,000 km^2 (100,000 mi^2) and consists of up to 4800 m (16,000 ft) of mostly Paleozoic strata in the Midwest Basins and Arches province (Barnes et al. 2009) (Fig. 1). The Michigan Basin is a roughly circular structural depression that includes the Lower Peninsula and eastern part of the Upper Peninsula of Michigan, eastern Wisconsin, northeastern Illinois, northern Indiana, northwestern Ohio, and western Ontario. The basin is bordered on the west by the Wisconsin Arch, on the south by the Kankakee Arch, and on the east by the Findlay Arch and Algonquin axis (Barnes et al. 2009).

Although the Michigan Basin contains deposits that range in age from the Precambrian to Cenozoic, the sedimentary record is dominated by Paleozoic sedimentary rocks (Catacosinos et al. 1990) deposited during several phases of subsidence (Sleep and Sloss 1978; Howell and van der Pluijm 1999). Basin subsidence initiated during the Precambrian and reached maximum rates during the Silurian to Middle Devonian as evidenced by the thick sedimentary deposits of this age (Howell and van der Pluijm 1999). The general shape of the Michigan Basin was established by the end of the Ordovician (Catacosinos 1973).

1.3. Lithostratigraphy

The Silurian rock record in the Michigan Basin is comprised of six lithostratigraphic groups, three of which are interpreted as having been deposited during the early Silurian period: Niagara Gr., Manistique Gr., and the BBG (Fig. 1). The BBG has been assumed to be an early Silurian unit

(Rhuddanian-Telychian) (Catacosinos et al. 2001). In the Michigan Basin, the BBG overlies the Cabot Head Shale (Cataract Gr.) and underlies the Schoolcraft Formation (Manistique Gr.).

The Burnt Bluff Formation is the name first proposed by Ehlers (1921) for carbonates outcropping along the Garden Peninsula in the UP. Ehlers (1921) defined the Byron Member (named by Chamberlin 1877, for the outcrops on the Door Peninsula near the town of Byron) and Hendricks Member, named by Smith (1915), for the exposures in the Hendricks Quarry in the eastern Upper Peninsula as members of Burnt Bluff Formation. Later, Cumings and Ehlers (1942) reclassified the Burnt Bluff Formation as the Burnt Bluff Group, and included the Hendriks and Byron Formations, both of which are dolomitic (Ehlers 1957). Ehlers and Kesling (1957) described the lithology, stratigraphy, and the internal structure of the Silurian strata of the Upper Peninsula of Michigan. They also mapped the lateral extent of the Silurian rocks from Garden Peninsula southwest to eastern Wisconsin and northeastern Illinois to northern Indiana; from Drummond Island to Cockburn and Manitoulin Island, then southeast to the region of Hamilton, Ontario and eastward to western New York (Fig. 2). This belt of BBG dips toward the center on the Michigan Basin (Howell and Pluijm 1999).

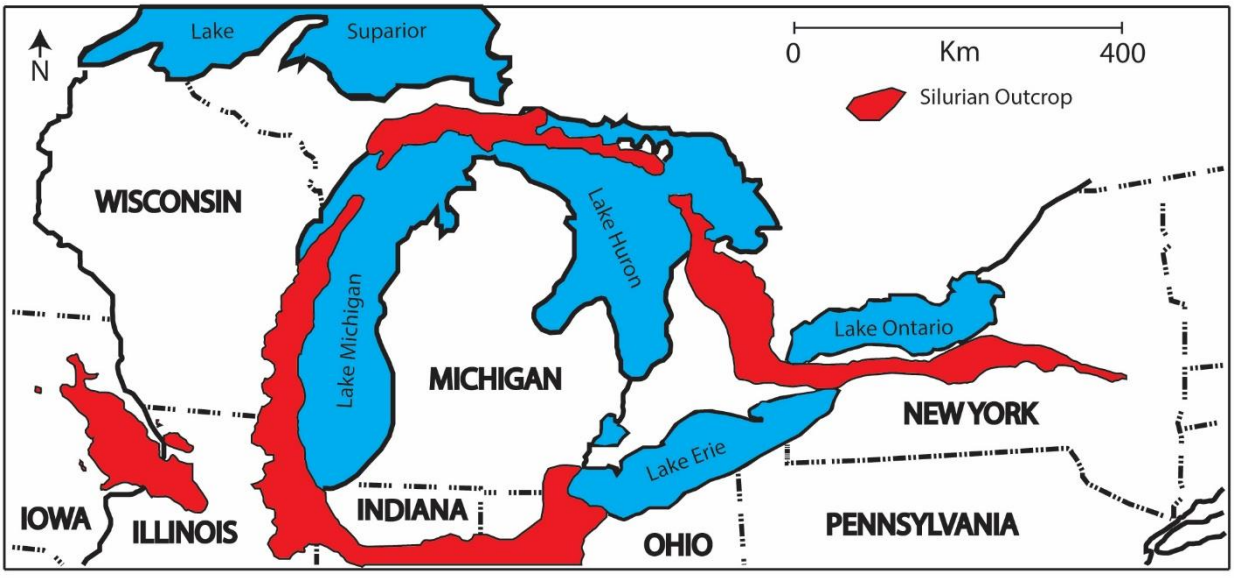

Figure 2: A map of the Great Lakes region illustrate the extent of the Silurian outcrops in New York, Ohio, Indiana, Illinois, Iowa, Wisconsin, Michigan, and Ontario. Modified after Ehlers and Kesling (1957).

Ehlers and Kesling (1957) focused on Silurian rocks in the Upper Peninsula of Michigan. They defined the Lime Island for the lower interval of the BBG in the Michigan Basin. Lime Island

was described as a cream-colored to buff, coarsely crystalline dolomite. Also identified was *Virginia* (Whiteaves), a diagnostic fossil of the Lime Island, which correlates to the upper part of the Mayville dolomite (Wisconsin) and Dyer Bay Dolomite of the Bruce Peninsula and Manitoulin Island, Ontario.

Ehlers and Kesling (1957) described the Byron in northern Michigan as a bedded, light to dark gray colored, crystalline dolomite, with scarce fossils. They described the Hendricks as gray to light gray, buff to light buff colored dolomite with lesser amounts of limestone, bedded to massive depending on the location. In addition to their descriptive work, Ehlers and Kesling (1957) mapped the three BBG formations in northern Michigan.

Johnson and Campbell (1980) identified three facies types in the BBG based on rock texture, faunal assemblages, and sedimentary structures, which were interpreted to represent unique depositional environments and water depths along a depositional profile. From shallowest to deepest, these environments include: 1) a peritidal carbonate mudflat characterized by fucoid-ostracods, and mud-dominated carbonates exhibiting fine laminations with mudcracks; 2) a shallow subtidal (above wave base) reef characterized by coral-algal boundstones composed of stromatolites, stromatoporoids, and tabulate corals; and 3) a deeper subtidal (below wave base) deposit characterized by brachiopods including Pentamerides such as: *Virgiana*, Pentamerus, and *pentameroids*. Johnson and Campbell (1980) used biofacies successions to interpret water depth changes within the studied section then constructed a relative sea level curve (Fig. 3).A pentameride brachiopod lineage was used for biostratigraphically dating the events with reference to the brachiopod succession in the Llandoverian type district of Wales.

Based on facies relationships in BBG carbonate outcrops, Johnson and Campbell (1980) constructed a relative sea level curve for the Lower Silurian. Johnson and Campbell (1980) described three transgressive and two regressive cycles in the BBG. The Pentamerid facies in the Lime Island was interpreted to represent sea level rise (whereas the Fucoid-Ostracod facies in the Byron and Hendricks represent sea level falls). A coral-algal community was identified at the contact between the Hendricks and Byron which was interpreted as a relative sea level rise (Fig. 3).

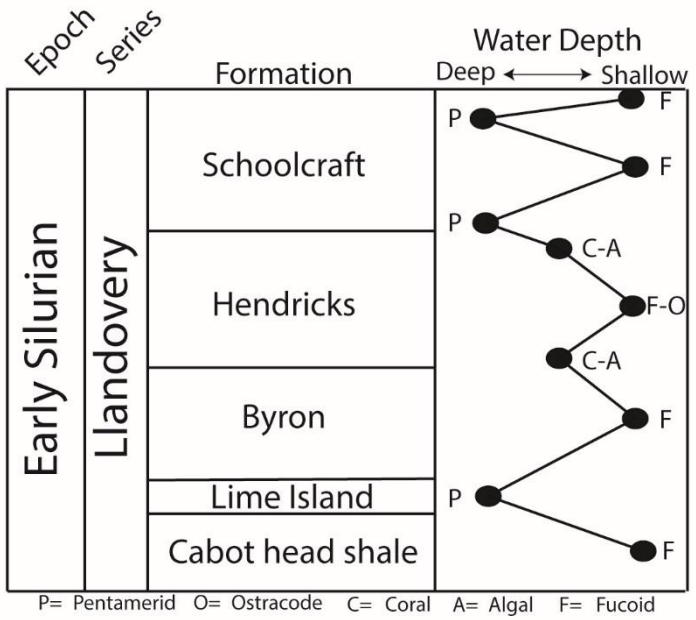

Figure 3: Relative sea level fluctuations interpreted for the Llandovery section in the Upper Peninsula of Michigan. Modified after Johnson and Campbell (1980).

Based on fossil content, sedimentary structures and facies stacking pattern, Harrison (1985) interpreted the depositional environment for each of the three formations of the BBG. Data was collected from outcrops in the Upper Peninsula and available cores in Lower Peninsula. The presence of abundant, large pentamerid brachiopods, lesser amount of molluscs, trilobites, corals and echinoderms, were used as evidence by Harrison (1985) to conclude that deposition of the Lime Island took place on a broad subtidal carbonate shelf. In contrast, the overlying Byron was interpreted as an intertidal-supratidal complex as evidenced by the presence of mudcracks and vertical dewatering structures present in thinly laminated algal mats. Based on the presence of laminar and digitate stromatoporoids, colonial rugose and tabulate corals, and solitary rugose corals, the Hendricks was interpreted by Harrison (1985) as a broad subtidal carbonate shelf containing small patch reefs. Harrison (1985) described the BBG in the central basin as an irregularly- bedded nodular lime mudstone with a limited assortment of sparse to abundant echinoderm ossicles. Based on these observations, Harrison (1985) interpreted the BBG in basin center to represent an outer shelf-continental slope deposit. More specifically, shelfal BBG facies grades laterally into UD-BBG in the basin center (Fig. 4).

Observations from core and wire-line logs suggest that the BBG thins to the south in the in the central Lower Peninsula, however, the BBG (the rocks in between the Cabot Head Shale and

Schoolcraft) exhibits a facies change to what has been called the UD-BBG. In the southeastern Lower Peninsula, a series of dolomitic shales, historically referred to as the "Clinton Formation" (an informal industry term in Michigan) have been identified (Catacosinos et al. 2001). These shales are generally positioned stratigraphically between the Cabot Head Shale and the overlying Manistique group (Ells 1962). The "Clinton Formation" has been suggested to be a distal equivalent of the BBG, but a clear stratigraphic relationship has not been established (Ells 1962; Harrison 1985; Voice et al. 2017).

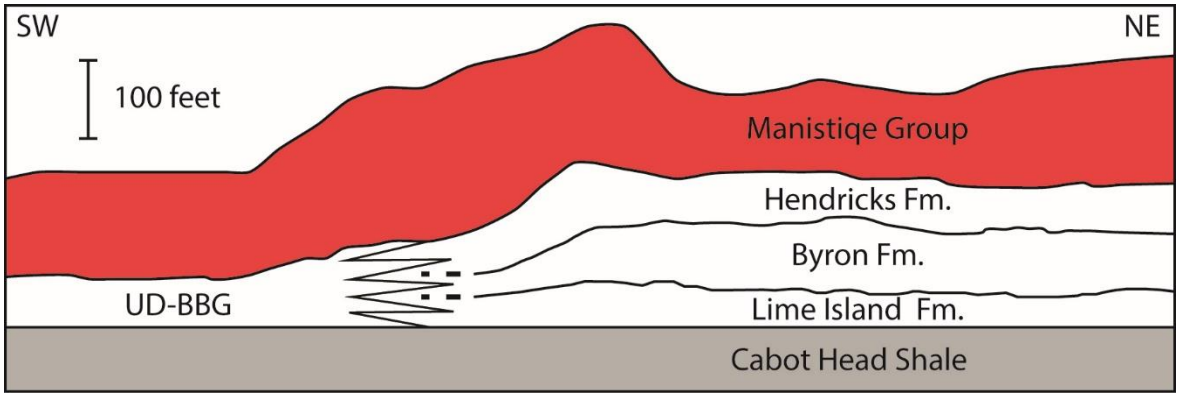

Figure 4: Lithologic cross section of the early Silurian units across the Michigan Basin. The diagram shows the current interpretation whereby the Lime Island, Byron, and Hendricks correlate with the UD-BBG in the basin center. Modified after Harrison (1985).

More recently, Watkins and Kuglitsch (1997) describe the BBG as southward-dipping ramp that extends from tidal-flat to deep water environments based on megafaunal and conodont biofacies of the BBG in northwestern Michigan Basin (Fig. 5). They described five distinct biofacies in core and outcrop samples. Each biofacies was interpreted to reflect one of the following depositional environments: 1) ostracod biofacies = tidal flat environment, 2) stromatoporoid-coral biofacies = shallow subtidal environments near fair-weather wave base, 3) crinozoan biofacies = subtidal environment 4) crinozoan-stromatoporoid biofacies = deeper subtidal environment, and 5) a crinozoan-sponge biofacies = the distal ramp environment.

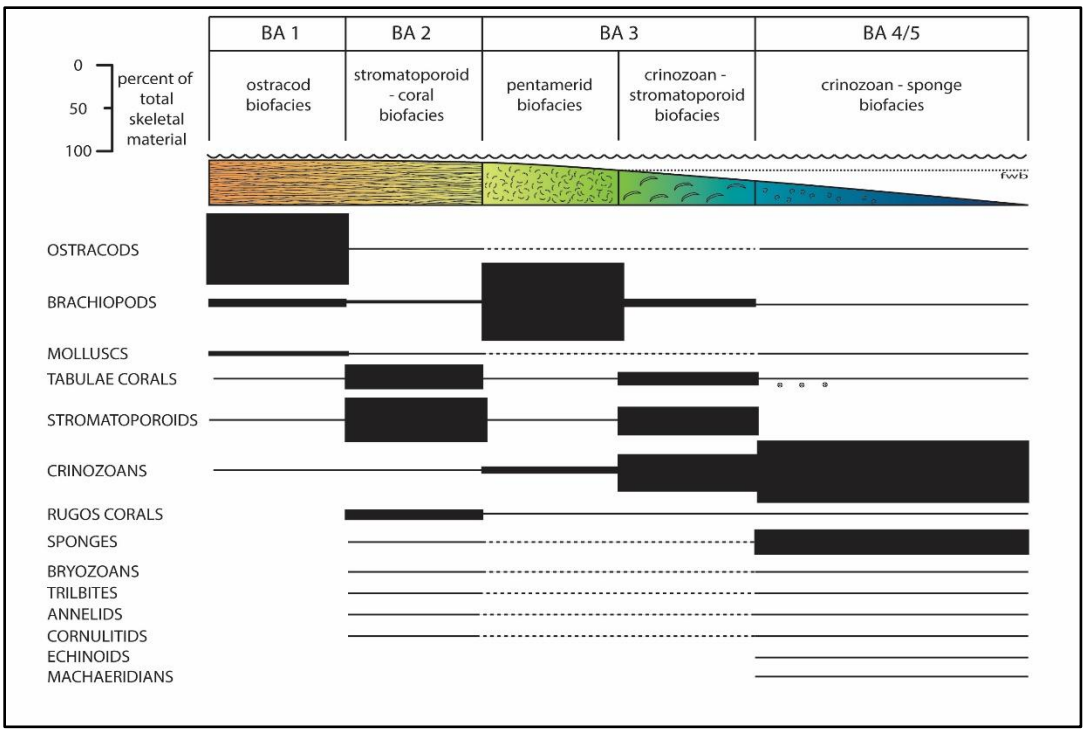

Figure 5: The relative abundances of the megafauna (biofacies) along the dip profile of the Michigan. Modified after Watkins and Kuglitsch (1997).

Voice et al. (2017) further refined the depositional environment models of Harrison (1985), and Watkins and Kuglitsch (1997) using additional data from core and outcrop in the Upper Peninsula of Michigan. Voice et al. (2017) identified sixteen distinct lithofacies facies – 14 in shelf positions and 2 in the central basin UD-BBG. Based on the observed facies, Voice et al. (2017) interpreted the depositional environment of the Lime Island as an open shelf located between fair-weather and storm weather wave base. He interpreted rocks of the Byron as tidal flat to restricted lagoon deposits, and the Hendricks as restricted lagoon to open shelf deposits. In the basin center, Voice et al. (2017) interpreted the UD-BBG as deep-water deposits below the fair-weather wave base (Fig. 6).

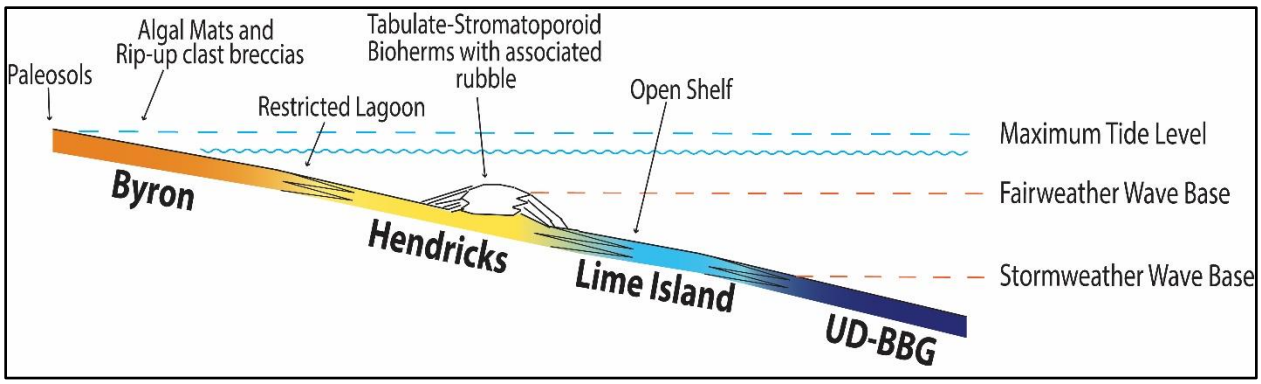

Figure 6: The depositional environments of the BBG units along a 2-D dip profile. Modified after Voice et al. (2017).

Previous attempts to describe the paleoenvironment of the BBG in the Michigan Basin (Ehlers and Kesling 1957; Johnson and Campbell 1980; Harrison 1985; Watkins and Kuglitsch 1997; Kuglitsch 2000; Voice at al. 2017), are based on lithostratigraphic and limited biostratigraphic observations. Therefore, chronostratigraphic correlation of the BBG across the Michigan Basin is not possible. In order to fully understand how the Michigan Basin evolved during BBG deposition, previous lithostratigraphic observations must be placed in a chronostratigraphic framework.

1.4. Biostratigraphy (Conodonts)

Conodonts are valuable index fossils that have been used to constrain the age of the Silurian stratigraphic column (Cooper 1980; Zhang and Barnes 2002; Bancroft et al. 2015; McAdams et al. 2017; Chen et al. 2017). However, there are only two biostratigraphic studies described conodonts from the BBG rock section in the Michigan Basin (Pollack et al. 1970; Kuglitsch 2000). Pollack et al. (1970) sampled one core from northwestern Michigan. The cored interval covers the section from Ordovician through Early Silurian rocks. The purpose of the study was to describe conodonts from Silurian strata. Results of this study suggest that BBG time of deposition is between Rhuddanian and Telychian.

Kuglitsch (2000) correlated Silurian rocks in the Michigan Basin area using conodonts collected from southeastern Wisconsin, northeastern Wisconsin, as well as the Upper Peninsula, and Lower Peninsula of Michigan. The samples collected from the Byron and Hendriks formations in northern Michigan Basin (well: Snowplow # 1-5) contained *Icriodella deflecta, Ozarkodina excavata , and Distomodus* sp. cf. D. *Kentuckyensis.* Based on the conodonts, Kuglitsch (2000)

interpreted the timing of deposition of the BBG in northern Michigan as Middle Aeronian. Samples collected from southern Michigan contained only Panderodus species. Panderodus is ubiquitous throughout the Silurian, therefore, it has no biostratigraphic value in constraining age of the BBG in the Michigan basin-center.

1.5. Chemostratigraphy

1.5.1. Carbon Isotopes Excursion (CIE)

In the last two decades, a number of Silurian age $\delta^{13}C_{carb}$ curves have been published for sedimentary basins all over the world (Patterson and Walter 1994; Azmy et al. 1998; Kump et al. 1999; Kaljo and Martma 2000; Kaljo et al. 2003; Cramer and Saltzman 2005; Melchin and Holmden 2006a; Loydell 2007; Munnecke and Mannik 2009; Cramer et al. 2011; Mclaughlin et al. 2013, McAdams et al. 2017). These $\delta^{13}C_{carb}$ records show abrupt and variably intensive positive and negative shifts from background values. These shifts, which are generally referred to as carbon isotope excursions (CIEs), have been independently age dated using a variety of methods including biostratigraphy, U-Pb geochronology, and Strontium isotopes. These studies collectively show that positive excursions occur within the same time period in different geographic locations. This suggest that these positive excursions represent global events that can be recorded in the different basins around the globe rather than a local event. Therefore, $\delta^{13}C_{carb}$ curves were used to solve different geological problems, particularly in stratigraphy and paleoclimatology.

The current study uses the $\delta^{13}C_{carb}$ curve, of the Llandovery age, to solve the stratigraphic problem of the BBG in the Michigan Basin. There are three positive excursions (Early Aeronian, Late Aeronian, and Valgu) and two negative shifts that were identified within the Llandovery age carbonate sections globally (Kaljo and Martma 2000; Kaljo et al. 2003; Cramer et al. 2011; Mclaughlin et al. 2013). However, the absolute values of these excursions and shifts are not the same in the different basins (Cramer et al. 2011). The Early Aeronian excursion is been recognized in the *Demirastrites triangulates* graptolite zone and Lower-middle *Aspelundia expansa* conodont zone (Cramer et al. 2011). The Late Aeronian excursion was recognized in the *Stimulagraptus sedgwickii* graptolite zone and the lower part of the *Distomodus staurognathodies* conodont zone (Cramer et al. 2011). The Valgu excursion was recognized in the

Streptograptus crispus graptolite zone and the lower part of the *pterospathodus eopennatus* conodont zone (Cramer et al. 2011). Based on previous biostratigraphic and lithostratigraphic studies, The BBG was deposited in the time interval from Upper Rhuddanian to Lower Telychian (Kuglitsch 2000).

1.5.2. $^{87}Sr/^{86}Sr$

Measurement of $^{87}Sr/^{86}Sr$ in biostratigraphically dated marine carbonates shows variation in $^{87}Sr/^{86}Sr$ between 0.707-0.709 during the Phanerozoic (McArthur 1994). Oceanic Sr has two sources, (i) the interaction between sea-water and oceanic crust, and (ii) weathering of the continental crust.. Oceanic crust $^{87}Sr/^{86}Sr$ can be low as 0.7029 (Palmer 1992), whereas weathered continental crust that reaches into the ocean via rivers can be as high as 0.712 (McArthur 1994). Variation of fluxes between these two sources is what produces changes $^{87}Sr/^{86}Sr$ of ocean water through time (McArthur 1994; Azmy et al. 1999). Therefore, $^{87}Sr/^{86}Sr$ variation through geological time is used as a proxy indicator of global tectonic evolution (Veizer et al. 1999). $^{87}Sr/^{86}Sr$ analysis of Llandovery age brachiopods and conodonts from localities around the world shows a range between 0.70793 and 0.70844 that progressively increase with time (Ruppel et al. 1998; Qing et al. 1998; Azmy et al. 1999). However, the age model that has been used to constrain ages of these $^{87}Sr/^{86}Sr$ values has uncertainty due to lack of biostratigraphic and chemostratigraphic data that can specify short time interval (Cramer et al. 2011). Most of the biostratigraphic data that were used to develop the age model of the $^{87}Sr/^{86}Sr$ values have a long-range time interval which increases the uncertainty.

Chapter 2
Methods

2.1. Geophysical Logs

Gamma Ray (GR) logs from over 250 wells that penetrate the entire BBG section were used in this study. GR log is used to determine the lithostratigraphic boundaries (formation tops) of the BBG three units as well as correlating these units across the Michigan Basin. Formation tops were used then to construct the structural and isopach maps of the different formations of the BBG.

2.2. Core Data and Core Analysis

In total, 18 cores were used in this study (table 1). The cores are housed at the Michigan Geological Repository for Research and Education (MGRRE). The cores that were used in this study were slabbed with a wet saw to help identify the different litho-facies. Cores were analyzed using a hand lens to differentiate lithology, fossil content, sedimentary structures, and to identify stratigraphic surfaces. Dilute hydrochloric acid (5% HCl) was used on core material to differentiate between limestone and dolomite. Thin section petrography and powder X-ray diffraction (XRD) were also used as necessary to determine mineralogy. The depositional textures of carbonate rocks observed in the core will be described in terms of the Dunham (1962) limestone classification.

Table 1: Cores in the BBG archived at the Michigan Geological Repository for Research and Education

Well Name	County	T.-R.	Permit #	Formation
Cousineau "A" #1-16	Alpena	16-29N-8E	37950	Cabot Head-Hendricks
Snowplow #4-6	Alpena	6-29N-5E	38243	Hendricks
Snowplow #1-5	Alpena	5-29N-5E	36758	Cabot Head Shale-Hendricks
Ford Scheuner #1-7	Alpena	7-31N-9E	31638	Cabot Head Shale-Hendricks
TH-75-2	Chippewa	3-41N-5E	481-752-317	Manitoulin Dolomite-Engadine
Lemcool #1	Grand Traverse	9-25N-10W	18512	Manitoulin Dolomite-Niagara Group
Johnson #1-6	Mecosta	6-16N-8W	36067	UD-BBG and Schoolcraft Formation
Whitney #1-17	Mecosta	17-15N-9W	43106	UD-BBG
St. Colfax and Knight #1-31	Mecosta	31-15N-9W	42264	UD-BBG and Schoolcraft Formation
Bruggers #3-7	Missaukee	7-24N-6W	34078	Byron and Hendricks Formations
Bradley #4	Newaygo	11-12N-13W	13816	Manitoulin Dolomite-Niagara Group
Altman #1-20	Newaygo	20-15N-11W	39166	UD-BBG
Islay Unit #1-22	Oceana	22-14N-18W	33154	Cabot Head Shale and UD-BBG
Schiller #1-10	Oceana	10-13N-18W	33134	UD-BBG and Schoolcraft Formation
Thompson #3-36	Osceola	36-17N-9W	36110	UD-BBG and Schoolcraft Formation
Wark #1-30	Osceola	30-17N-8W	35977	UD-BBG and Schoolcraft Formation
Consumers Power #1-3	Oscoda	3-26N-1E	37145	Cabot Head Shale-basal Hendricks
Cooks #1	Schoolcraft	19-41N-17W	NA	Trenton- Byron

2.3. Biostratigraphic Data (Conodonts)

Two cores were sampled for conodonts. The first core was the Lemcool #1. The cored interval for the Lemcool #1 was 7262-6964 ft measured depth from the ground level (total thickness = 298 ft). This core covers the Cataract Group, the BBG, and the Manistique Group. In total, 100 samples were collected from the Lemcool #1 at a 3 ft. sampling rate. Each sample collected weighed 1 kg. The second well sampled was the Freudenberg #1-31. The cored interval of this well is 8180-8118 ft (total thickness = 72 ft). The Freudenberg #1-31 covers the UD-BBG and the lower part of the Manistique Group. In total, 65 samples were collected from the Freudenberg #1-31. The Freudenberg #1-31 had less core material available for sampling, so a smaller amount of 0.5 kg per sample was used. All conodont samples were prepared following

the methods described in Kuglitsch (1999). The methods are summarized as follows: Bulk rock samples were dissolved using a solution of ≤12% acetic acid. Residues were separated into heavy and light fractions using separation funnels and tetrabromoethane. Conodonts, and other phosphatic microfossils were extracted from the heavy fraction using a wetted artist's brush.

2.4. Stable Carbon Isotopes

Four wells were selected for carbon isotope analyses (Snowplow #1-5, Snowplow #4-6, Lemcool #1, Johnson #1-6). In total, ~300 samples were collected and analyzed for $\delta^{13}C_{carb}$ and $\delta^{18}O_{carb}$ at the University of Michigan Stable Isotope Lab. In the Lemcool# 1 core, 100 samples were collected from Manitoulin Formation, Cabot Head Shale, Lime Island, Byron, Hendricks, Schoolcraft and Cordell at 3' sampling rate. The Snowplow# 1-5 core, 55 samples were collected from Cabot Head Shale, Lime Island, Byron and Hendricks at 3' sampling rate. The Snowplow #4-6 core, 21 samples were collected from the Hendricks and Schoolcraft at 3'sampling rate. The Johnson# 1-6 core, 91 samples were collected from the UD-BBG and the Manistique Group at 1' sampling rate. An average of 0.5 grams of powdered carbonate was collected using a rotary drill equipped with a tungsten carbide drill bit. Stable isotope analyses were performed according to standard methods (Caruthers et al. 2018). These methods are summarized as follows: Carbonate samples weighing a minimum of 10 micrograms are placed in stainless steel boats. Samples are then transferred to individual borosilicate reaction vessels and reacted at 77° ± 1°C with 4 drops of anhydrous phosphoric acid for 8 minutes (12 minutes for dolomites, 17 minutes for apatite, and 22 minutes for siderites) in a Finnigan MAT Kiel IV preparation device coupled directly to the inlet of a Finnigan MAT 253 triple collector isotope ratio mass spectrometer. O^{17} corrected data are corrected for acid fractionation and source mixing by calibration to a best-fit regression line defined by two NBS standards, NBS 18 and NBS 19. Data are reported in ‰ notation and are reported relative to Vienna Pee Dee Belemnite (VPDB).

2.5. $^{87}Sr/^{86}Sr$

Seven conodonts samples were analyzed for $^{87}Sr/^{86}Sr$ at the Ohio State University Thermal Ionization Mass Spectrometer (TIMS) Laboratory using the method of Saltzman et al. (2014) (table 2). Four samples were selected from the Lemcool #1 core and three samples from the Freudenberg #1-31 core. To prepare the separated conodont elements for isotopic analysis,

~0.2 mg of the conodont elements were sonicated three times in Milli•Q ultrapure water and digested in 6N distilled hydrochloric acid with an agitator and centrifuge before being left to sit for 12 hours at room temperature. Samples not fully digested were subjected to additional processing via agitator, centrifuge, and sonication. An aliquot of the digested sample was taken for analysis of Sr concentration using inductively coupled plasma mass spectrometry (ICP-MS).

Two samples were run in duplicate, one leached and one unleached. Unleached samples were processed as described above. Leached samples were sonicated three times in Milli•Q ultrapure water before being placed in 0.5 mL 5% acetic acid overnight (~12 hours) at room temperature (~25 °C). Leached samples were rinsed three times with Milli•Q ultrapure water and digested in 6N distilled hydrochloric acid as described above. Instrumental mass fractionation during analyses was corrected by normalizing measured ratios to $^{88}Sr/^{86}Sr = 8.3752$ using an exponential law. Replicate analysis of standard reference material (SRM) 987 yielded 0.710263 ± 0.000004 (2σ, N=3). Sample $^{87}Sr/^{86}Sr$ data from the TIMS were normalized to SRM 987, which has a reported value of 0.710245. On the TIMS, Sr was ionized using a Re single filament with Ta_2O_5 activator. Prior to TIMS measurements, each Sr sample was evaporated to dryness and reconstituted in 1 µL of 1 N HNO_3. To load the sample onto TIMS filaments, 0.5 µL Ta_2O_5 activator was added to a rhenium ribbon single filament and heated to near dryness at a current of 0.6 A. Then, the 1 µL sample solution containing 0.5-1 µg of Sr was added to the filament and heated to dryness at the same current. Another 0.5 µL of Ta_2O_5 activator was added and heated to dryness at the same current. The current was then increased to 1.8 A for 1 minute and then slowly increased again until the filament glows dull red. Sr isotope ratios were measured in static mode using the cup configuration using 200 sets of cycles, taken in 10 blocks with a beam intensity of ~4 V for ^{88}Sr (Table 2).

Chapter 3
Results

3.1. Lithofacies and Gamma Ray

The stratigraphic interval examined in this study consists of the Cabot Head Shale, the Burnt Bluff Group, and the Manistique Group. The Cabot Head Shale is characterized by a green to dark gray shale to shaley carbonate. The range of GR is between 120-130 API (Fig. 7). The Burnt Bluff Group is comprised of three lithological units. The Lime Island Formation is composed of burrowed mudstone interbedded with skeletal wackestones and packstones (Appendix A and D). In contrast to the high values of the Cabot Head Shale, GR values for the Lime Island range between 0 and 10 API (Fig. 7). The Byron is composed of light gray to buff, laminated dolo-mudstones and dolo-wackestones (Appendix A and E). Some intervals of the Byron are not dolomitized, and skeletal fragments are generally rare. The GR of the Byron ranges between 40 and 60 API, and is the highest among the three units of the BBG (Fig. 7). The Hendricks is composed of skeletal packstone to grainstones with abundant tabulate corals and brachiopods (Appendix A and F). The GR signature of the Hendricks ranges between 10 and 30 API. The Manistique Group is composed of two formations: the Schoolcraft and Cordell. The Schoolcraft is composed of gray to dark gray, mudstone to wackestone, chert is abundant in this formation. The range of GR of the Schoolcraft is between 40 and 60 API (Fig. 7). The Cordell is characterized by the presence of the chert nodules intervals. The GR of the Cordell range between 80-100 API. As mentioned above, GR was used to identify the lithostratigraphic boundaries of the BBG in the Michigan Basin. These boundaries then used to construct the structural and isopach maps of the BBG (Fig 8 and Fig 9). The Isopach map show that the BBG is represented by thick interval in northern Michigan (250-300 ft) and starts to thin toward central Michigan (20-30 ft).

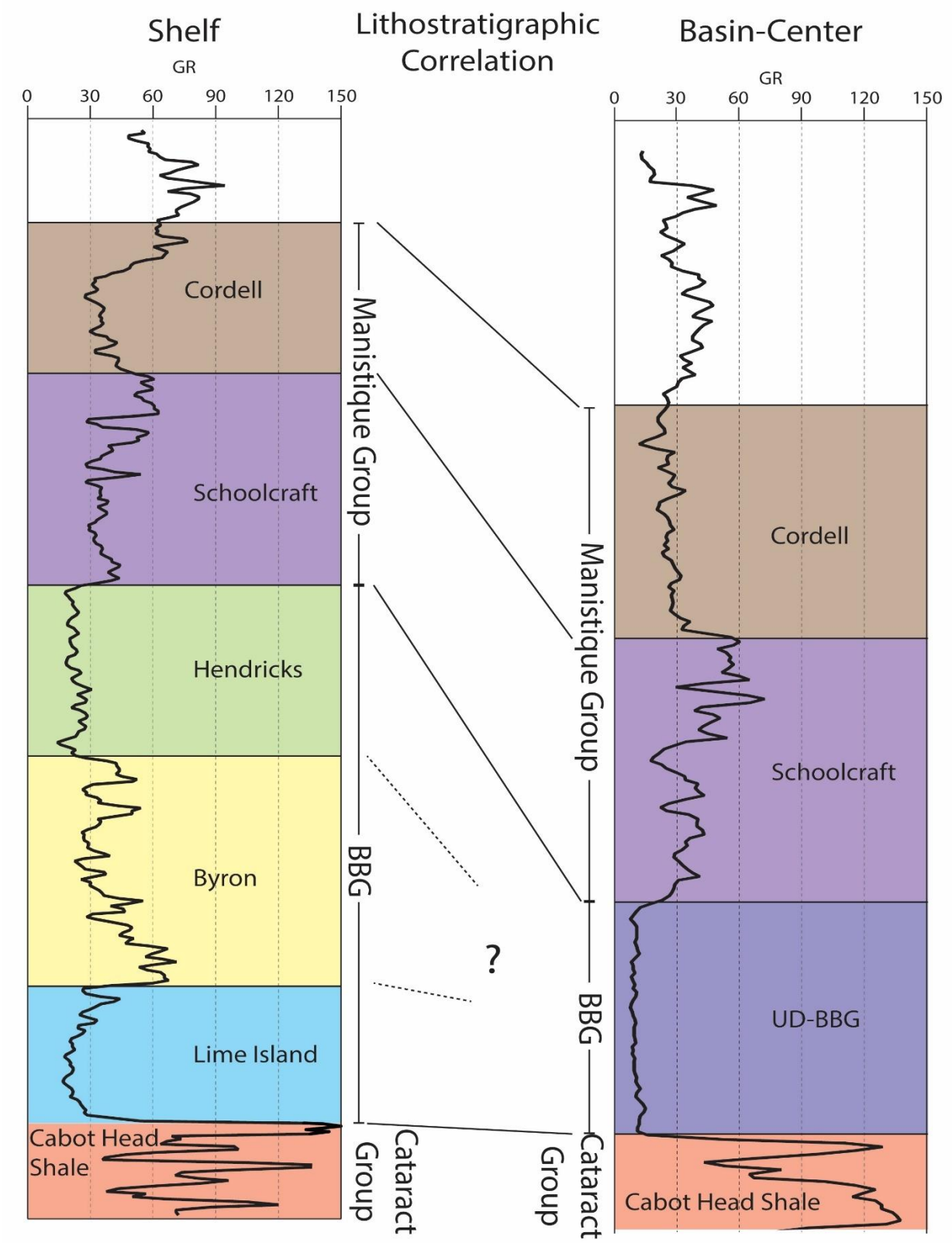

Figure 7: The interpreted GR log signatures that are used to identify and correlate the stratigraphic intervals of interest both in the shelf and basin-center.

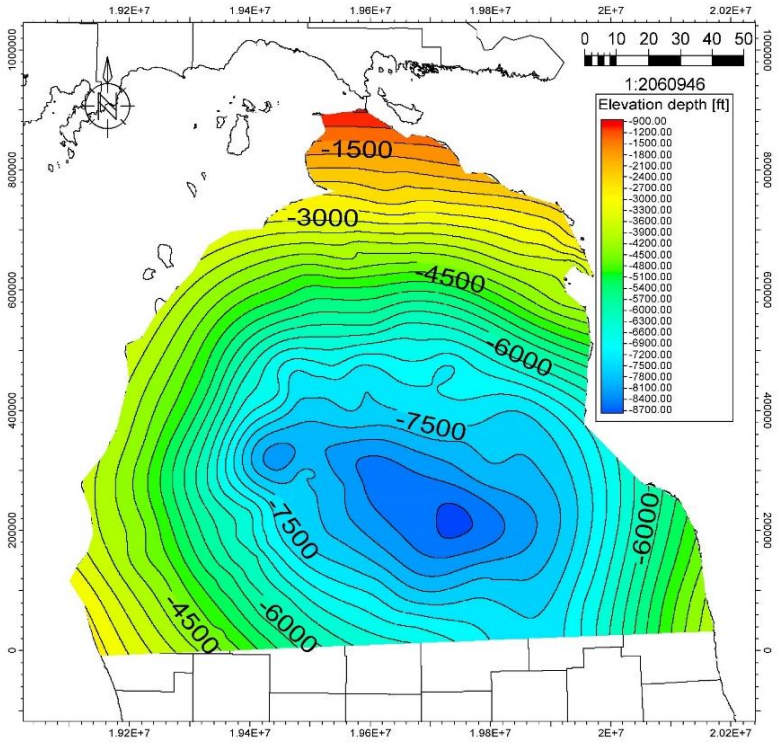

Figure 8: Top of BBG structural map.

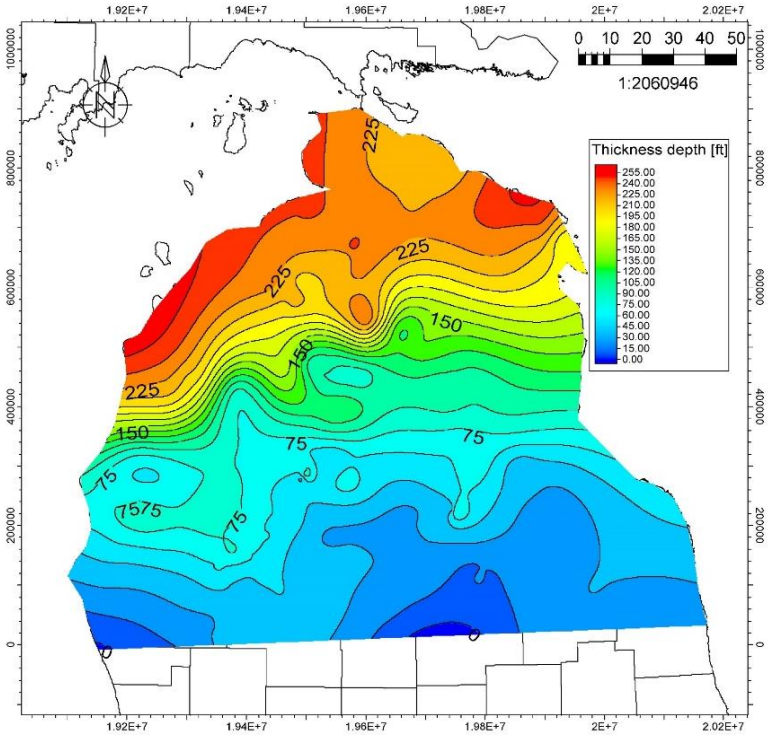

Figure 9: BBG isopach map

3.2. Carbon isotopes ($\delta^{13}C_{carb}$)

Results from over 350 $\delta^{13}C_{carb}$ analyses show a broad range of values between 0.7‰ and +5.07‰ VPDB (Table 3). The cross-plot of exhibits no clear correlation between $\delta^{13}C_{carb}$ and $\delta^{18}O_{carb}$Fig 10). Overall, the correlation coefficient of all data plotted together is ~ 0.002, whereas, the correlation coefficient of the data plotted by well is < 0.1. The baseline values of the non-excursion $\delta^{13}C_{carb}$ in all five wells range between 0.5-1.3‰. In terms of stratigraphic variability, the carbon isotope data show a number of isotope excursions within the core profiles, which are generally smooth with low sample to sample volatility. Carbon isotope excursions (CIEs) show a slight shift in their absolute values in the different location with the basin. For example, the CIEs show higher values towards the shelf and lower values toward the basin-center. In the Lemcool #1 well, $\delta^{13}C_{carb}$ results show three positive excursions of +2.5‰, +5‰, +3‰, at 7235-7115 ft, 7055-7015 ft, and 6970 to 6950 ft, respectively. A negative excursion of -0.5‰ at 7015-7000 ft is also observed (Fig. 11). Though $\delta^{13}C_{carb}$ values range from +0.5‰ to +2‰, results from the Snowplow #1-5 show no major excursions (Fig. 12). Results from the Snowplow #4-6 show a positive $\delta^{13}C_{carb}$ excursion of +3‰ at 5570-5530 ft and a negative excursion of -0.7‰ at 5530-5525 ft (Fig. 12). Data from the Johnson #1-6 well show two positive excursions; the first a +3‰ shift at 8109-8112 ft depth and the second ranges between +1.5 and +2‰ located at 8154-8194 ft (Fig. 13).

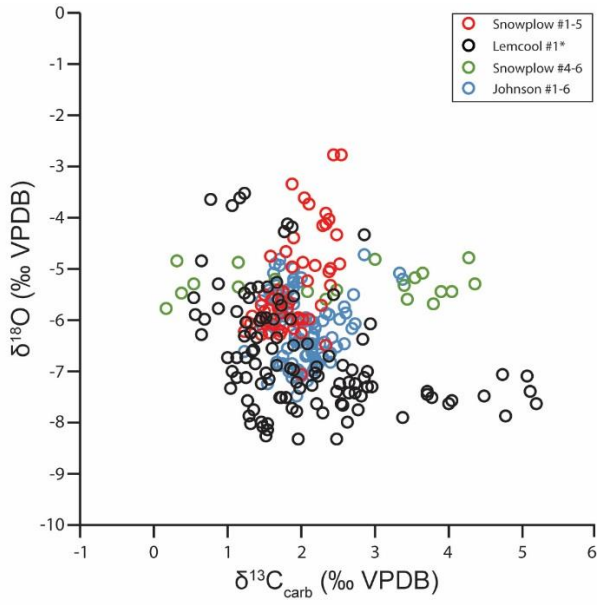

Figure 10: Cross-plot of $\delta^{18}O_{carb}$ vs. $\delta^{13}C_{carb}$

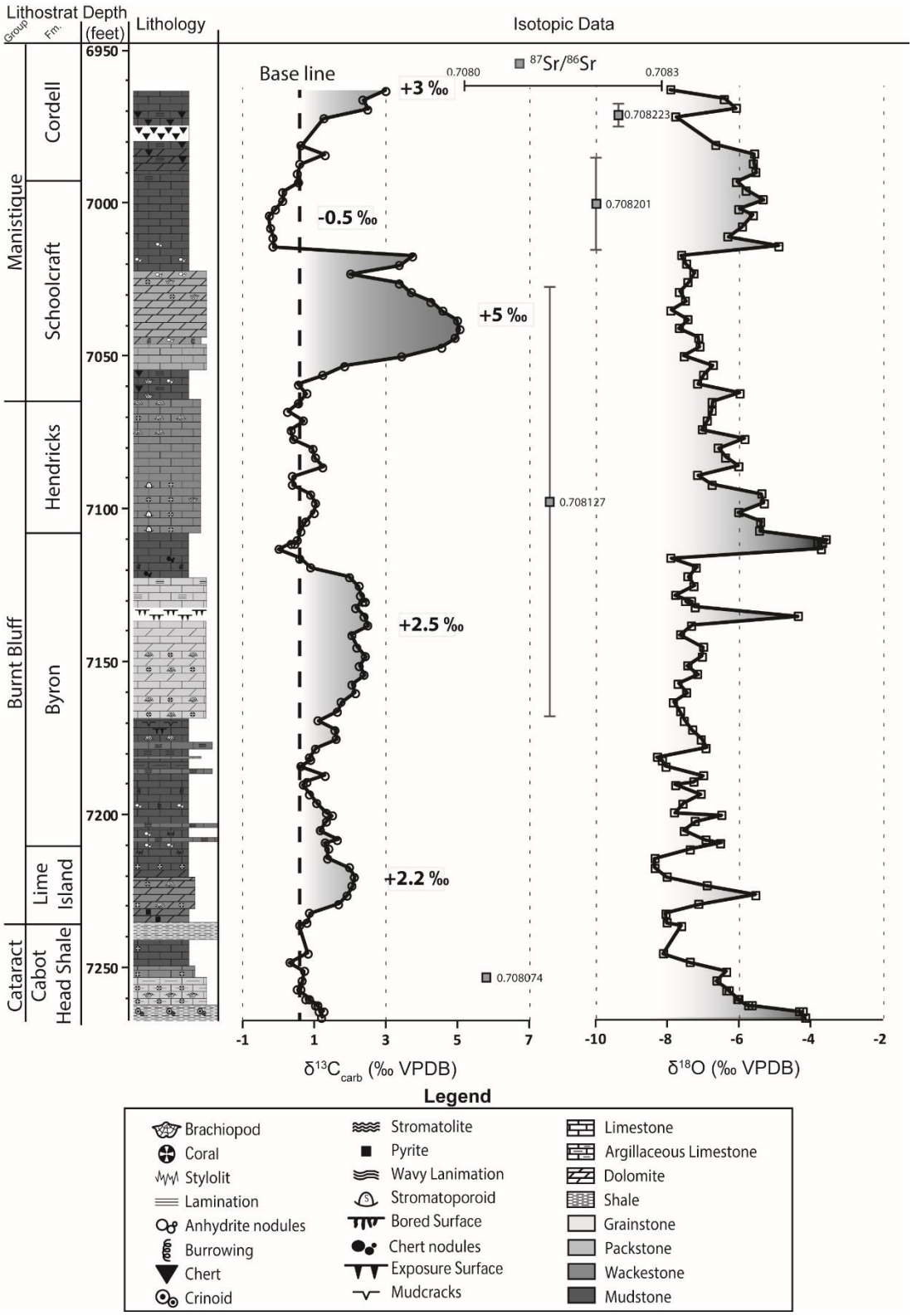

Figure 11: $\delta^{18}O_{carb}$, $\delta^{13}C_{carb}$, $^{87}Sr/^{86}Sr$, and facies profile of the Lemcool #1 core.

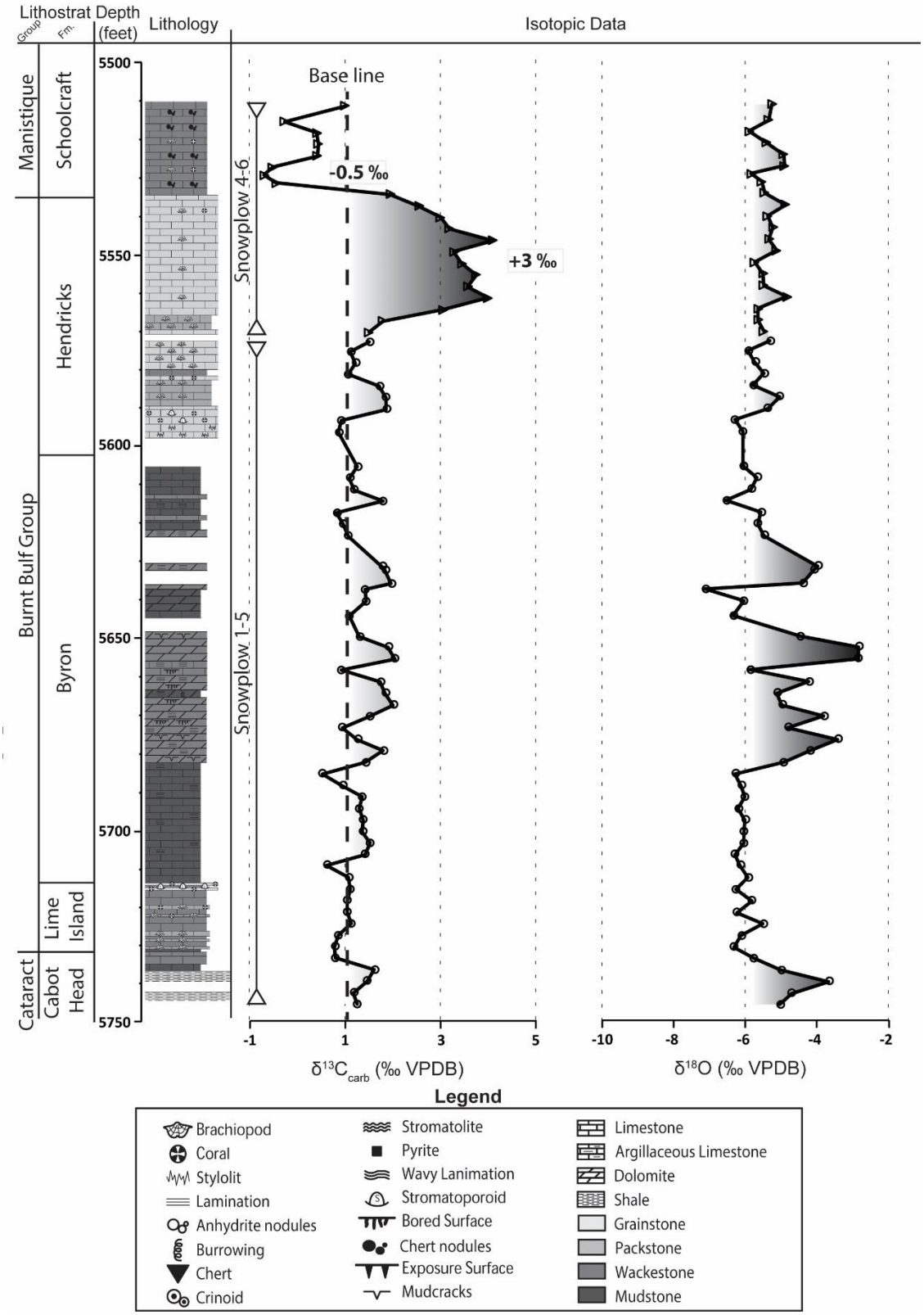

Figure 12: $\delta^{18}O_{carb}$, $\delta^{13}C_{carb}$, and facies profile of the Snowplow #1-5 and Snowplow #4-6 cores.

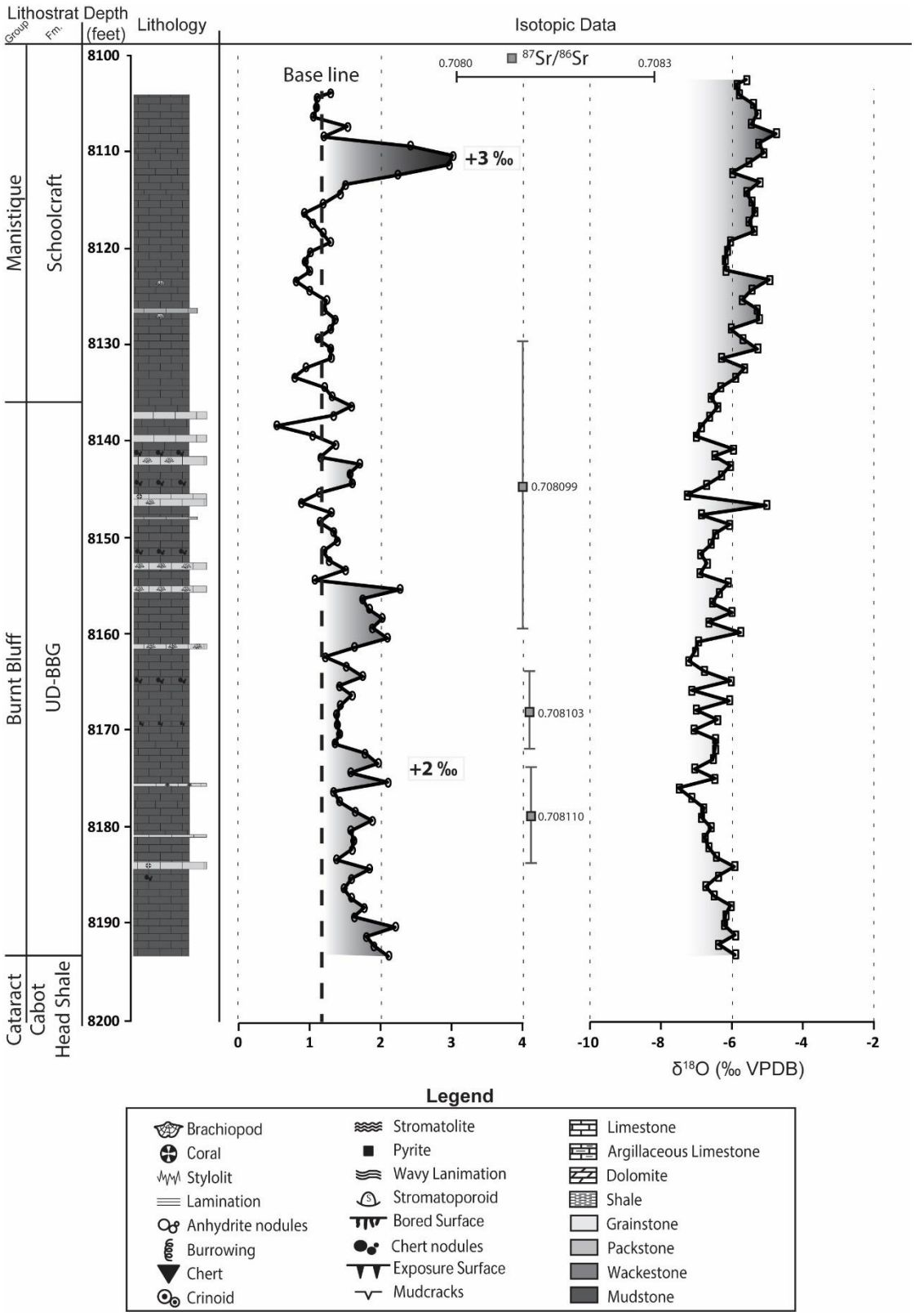

Figure 13: $\delta^{18}O_{carb}$, $\delta^{13}C_{carb}$, $^{87}Sr/^{86}Sr$, and facies profile of the Johnson #1-6 core.

3.3. Conodont biostratigraphy

Pa elements from the conodont *Aulacognathus bullatus* and what may be *Ozarkodina policlinata* were collected from the upper section of the Schoolcraft in the Lemcool #1 core at 6973.4 ft depth. These conodonts were reviewed and confirmed by Jeffrey J. Kuglitsch and Alyssa M. Bancroft. All other dissolved rock samples from the Freudenberg #1-31 and Lemcool #1 wells contained *Panderodus* sp., which is primarily a long time-range coniform species with no time significance. The conodonts with no biostratigraphical significance were used for $^{87}Sr/^{86}Sr$ analyses.

3.4. Strontium isotopes ($^{87}Sr/^{86}Sr$)

With respect to the $^{87}Sr/^{86}Sr$ results, the data show broad variation through the stratigraphic profiles (Table 2). In general, $^{87}Sr/^{86}Sr$ values decrease with depth in both wells. $^{87}Sr/^{86}Sr$ values in the Lemcool #1 range between 0.708049 and 0.708240 over the 7245.2-6974.6 ft depth interval (Fig. 11). $^{87}Sr/^{86}Sr$ data in the Freudenberg #1-31 range between 0.708099 and 0.708110 over the 8123.5 ft depth interval (Fig. 13).

Table 2: $^{87}Sr/^{86}Sr$ results

Well	Depth (ft)	Measured $^{87}Sr/^{86}Sr$	1σ	Normalized $^{87}Sr/^{86}Sr$	2σ
Lemcool #1	7245.2	0.708067	3.01E-06	0.708049	*6.01E-06*
Lemcool #1	6967.2-6974.6	0.708257	3.10E-06	0.708240	*6.21E-06*
Lemcool #1	7027-7169.5	0.708145	3.04E-06	0.708127	*6.09E-06*
Lemcool #1	8985.6-7016	0.708219	3.06E-06	0.708201	*6.11E-06*
Freudenberg #1-31	8155.3-8166.8	0.708121	2.61E-06	0.708103	*5.22E-06*
Freudenberg #1-31	8168.7-8179.3	0.708128	4.00E-06	0.708110	*7.99E-06*
Freudenberg #1-31	8123.5-8151	0.708116	2.73E-06	0.708099	*5.46E-06*

Chapter 4
Discussion

4.1. CIEs as Global Time Horizons

A number of different geological processes can impact the carbon isotope record preserved in the BBG. The identification of the CIEs in multiple basins around the world within coeval rock sections has lead previous researchers to conclude that they reflect primary depositional signatures that represent global perturbations in the carbon cycle (Patterson and Walter 1994; Azmy et al. 1998; Kump et al. 1999; Kaljo and Martma 2000; Kaljo et al. 2003; Cramer and Saltzman 2005; Melchin and Holmden 2006a; Loydell 2007; Munnecke and Mannik 2009; Cramer et al. 2011; McLaughlin et al. 2013, McAdams et al. 2017; Caruthers et al. 2018). As such, CIEs are routinely used for correlation purposes. Others (Ahm et al. 2018) contend, however, that CIEs reflect local diagenesis, and are therefore not reliable for correlation. Because the current study uses the observed CIEs as timelines for stratigraphic correlation, it is of value to discuss the key observations that suggest CIEs do not reflect diagenesis. First, CIEs occur in both limestone and dolomite, and more importantly, perhaps, cross limestone-dolomite contacts. Given that dolomite is the most pervasive diagenetic product in the BBG, it is reasonable to expect that carbon isotope record might be impacted by the dolomitization process. The observations show that carbon isotope excursions are not related to dolomitization. This observation is supported by the poor correlation between the $\delta^{13}C_{carb}$ and $\delta^{18}O_{carb}$. The $\delta^{18}O_{carb}$ is easily reset due to the high abundance of oxygen in the sea water and pore fluid whereas carbon isotope values are considered as the most diagenetically robust of the geochemical systems due to the high concentration of carbon in carbonate rocks and low concentration of carbon in the sea water and pore fluid (Ahm et al. 2018). The poor correlation between $\delta^{13}C_{carb}$ and $\delta^{18}O_{carb}$ suggest that the dolomitization process did affect the carbon isotopic record. Second, CIEs are identified in different lithofacies in the different positions (i.e. shelf, slope, basin-center) across the Michigan Basin. This is evidence that the carbon isotopic record of the rocks is independent of the depositional environment. More specifically, CIEs occur in shallow and deep water settings. Lastly, the $\delta^{13}C_{carb}$ curves presented here are very similar to the composite global $\delta^{13}C_{carb}$ curve of Cramer et al. (2011), which suggests that they are not local diagenetic signatures. Furthermore, Caruthers et al. (2018) studied the Late Silurian section in

the Michigan Basin and showed that the organic carbon record and the carbonate record were the same. This suggest that the CIEs in the carbonate record are not result of diagenesis.

4.2. Age Constraints

Although biostratigraphy is commonly used to constrain the ages of lithologic units worldwide (e.g., Pollack et al. 1970; Cooper 1980; Zhang and Barnes 2002; Bancroft et al. 2015; McAdams et al. 2017, Chen et al. 2017), its use in core studies is limited by the low abundance of rock material that can by dissolved to obtain age-diagnostic fossils. Therefore, this study uses an integrative approach that utilizes multiple lithological and geochemical datasets, in addition to biostratigraphy, to constrain the ages of the different BBG units across the Michigan Basin. (i)

Based on observed lithological and biological changes of the BBG in the Michigan Basin from north to south (Harrison 1985; Voice et al. 2017), this study has subdivided the Michigan Basin during the BBG deposition time into three physiographic positions along the 2-D dip profile, shelf, slope, and basin-center (Fig. 14). The shelf position in the basin corresponds to the southern Upper Peninsula and northern Lower Peninsula. In this position, the Lime Island, Byron and Hendricks can be identified using GR and core description (Fig. 7; Appendix D, E, and F). The Lime Island in shelf position (Appendix D) is characterized by a gray to dark gray, nodular mudstone that interpreted to be formed in a deep-water open marine environment. This facies in the Lime Island is interbedded with thin skeletal grainstones that is interpreted as storm deposits (Voice et el. 2017). The Byron in the shelf position (Appendix E) is characterized by light gray to buff, laminated mudstone, mud-cracks and exposure surfaces are abundant. Byron facies are interpreted to be deposited in restricted to nearshore shallow subtidal to supratidal environment above the fairweather wave base (Voice et al. 2017). The Hendricks in the shelf position (Appendix F) is interpreted, based on the presence of tabulate corals and brachiopods (Appendix A and F), to be deposited in shallow water environment below the fairweather wave base and above the stormweather wave base (Voice et al. 2017). In the slope position, however, the three formations that comprise the BBG are difficult to distinguish due to distinct facies change to a deeper-water environment. The slope is defined as topographic transition between flat lying shallow shelf and the deeper basin-center. Toward basin-center in the south, the BBG is represented by the UD-BBG. UD-BBG is composed of gray to dark gray, nodular mudstone facies

that is interpreted to be formed in a deep water environment below the storm weather wave base. The Lime Island, Byron, and Hendricks cannot be distinguished in this position (Fig. 7).

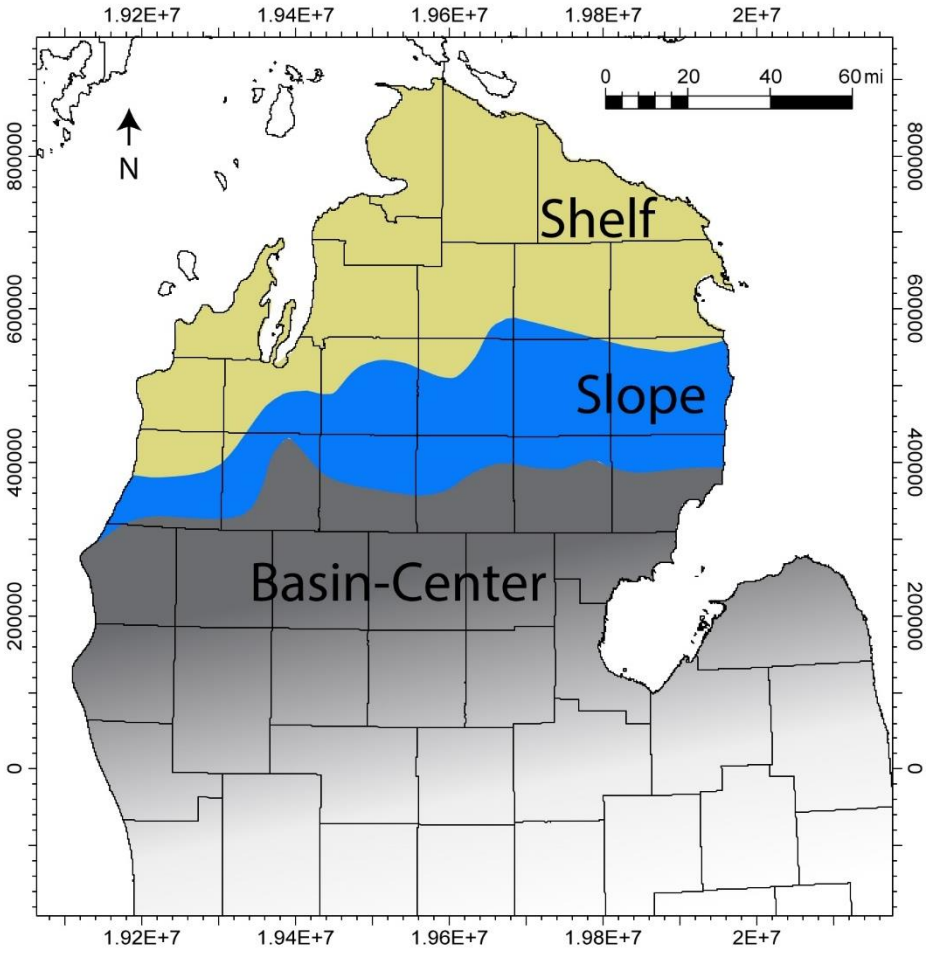

Figure 14: A paleogeographic map that is based on thickness and facies observations show the geographical distribution of the BBG's depositional environments.

The shelf position (Fig. 14) is characterized by two cores, the Snowplow #1-5 and the Snowplow #4-6, which are separated by a distance of less than 0.5 mile. When combined, these cores cover the section from upper Cabot Head Shale to the lower Schoolcraft. Based on the conodonts *Icriodella deflecta, Ozarkodina excavata, and Distomodus* sp. cf. D. *Kentuckyensis* that were identified in the Byron and lower Hendricks Formations in the Snowplow #1-5 core, Kuglitsch (2000) interpreted the age of the BBG in the shelf position as Middle Aeronian. The composite $\delta^{13}C_{carb}$ curve for the Snowplow #1-5 and Snowplow #4-6 shows a positive excursion (+3‰ VPDB) in the upper section of the Hendricks that underlies a negative shift (-0.5‰ VPDB)

at the bottom of the Schoolcraft (Fig. 12). The interpretation of Kuglitsch (2000) suggests that the positive CIE is the Late Aeronian excursion (Cramer et al. 2011). Given this, the age of the upper section of the Hendricks is interpreted to be late Aeronian (Ae3; *S. sedgwickii*) whereas the lower section of the Schoolcraft is interpreted to be early Telychian (*Te1; Sp. guerichi*) (Cramer et al. 2011). The early Aeronian excursion was not identified in this well, therefore, the lower section of the Hendricks, Byron, Lime Island and upper section of the Cabot Head Shale are interpreted to represent middle Aeronian age (Ae2; *M. argenteus/Pr. Leptotheca – L. convolutus*) (Fig. 15).

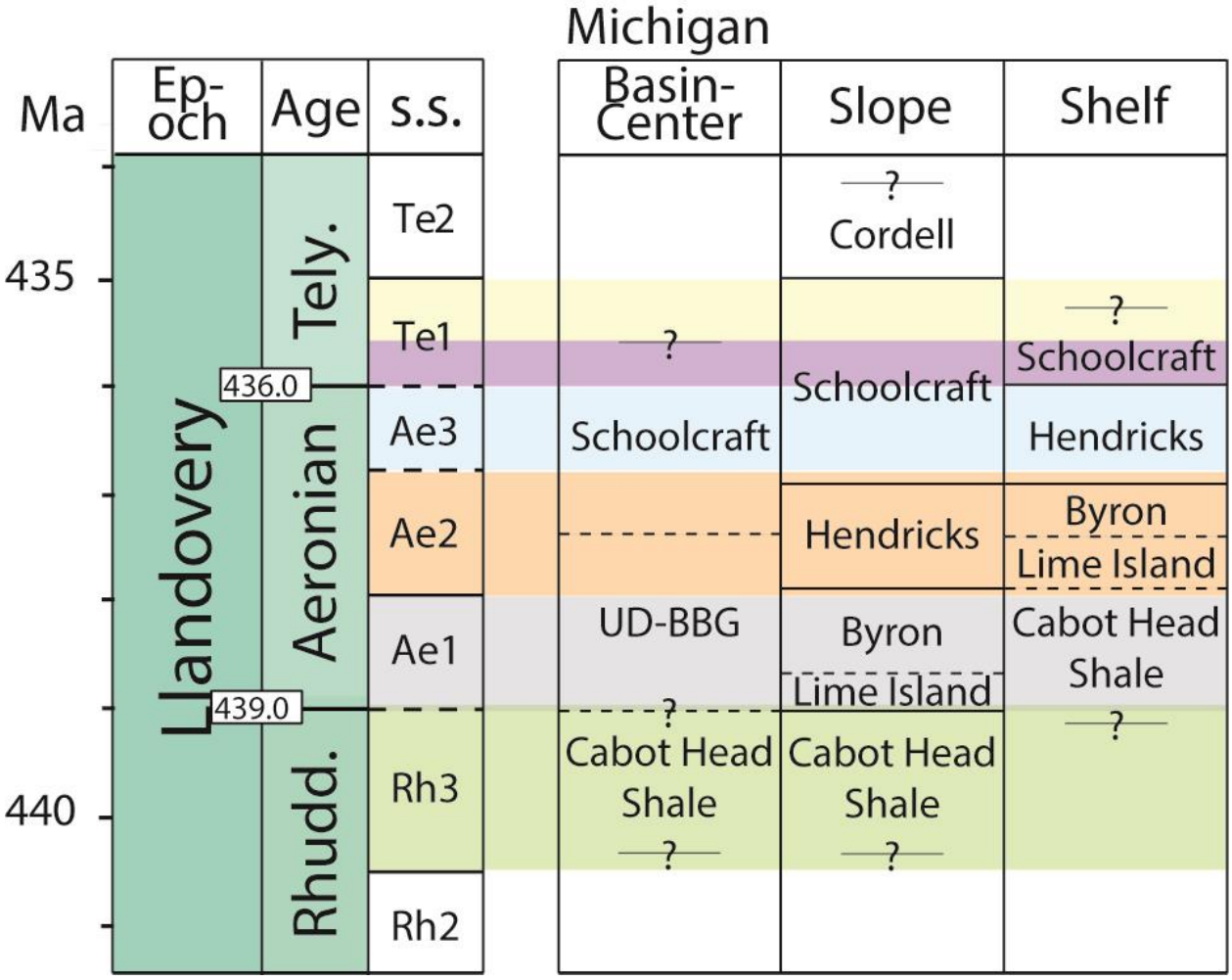

Figure 15: The diagram shows the revised ages of the BBG's units in the in the different locations around the Michigan Basin.

The slope position (Fig 14), a transitional environment between shallow water environment (shelf) and deep-water environment (basin-center), was represented by the Lemcool #1, Bruggers #3-7, and Consumer Power #1-3 cores in this study. Based on the

conodonts identified in the Bruggers 3-7 and the Consumer Power #1-3, Kuglitsch (2000) interpreted the age of the BBG in these two cores as Aeronian. Conodont results from the Lemcool #1 core in the lower section of the Cordell Formation include *Aulacognathus bullatus,* which is significant because the first reported occurrences are within the *Pt. eopennatus Superzone*. This observation is consistent with an age of Lower Telychian (Te2) for the lower Cordell in the Lemcool #1 core.

The $\delta^{13}C_{carb}$ curve from the Lemcool #1 slope core shows three positive carbon isotope excursions (Fig. 11). From bottom to top these include: (i) a 2.2-2.5‰ excursion that spans from the bottom of Lime Island to the top of the Byron; (ii) a 5‰ excursion that spans from the top of the Hendrick to the middle of the Schoolcraft; and (iii) a +3‰ excursion that spans from the top of Schoolcraft and through the lower section of the Cordell (i.e. the uppermost unit of the Manistique). The distinctive $\delta^{13}C_{carb}$ curve shape in the Lemcool #1 is very similar to the published generalized $\delta^{13}C_{carb}$ global curve of the Llandovery (Cramer et al. 2011). The $^{87}Sr/^{86}Sr$ values of this study (Fig. 16) also constrain the lower $\delta^{13}C_{carb}$ excursion (2.2-2.5‰) to the Early Aeronian global excursion of Cramer et al. (2011) and the middle excursion (+3‰) to the Late Aeronian excursion (Cramer et al. 2011). Lastly, the index conodont *Aulacognathus bullatus* is coincident with the uppermost positive excursion (+3‰) identifying it as the Valgu excursion (Cramer et al. 2011). Taken together with the lithostratigraphic information, the $^{87}Sr/^{86}Sr$ and conodont data suggest that ages of the lithostratigraphic units in the Lemcool #1 core are the following: Cabot Head Shale age is Rh3, Lime Island and Byron ages are Ae1, Hendricks age is Ae2, Schoolcraft age is Ae3 to Te1, and lower Cordell age is Te2 (Fig. 15).

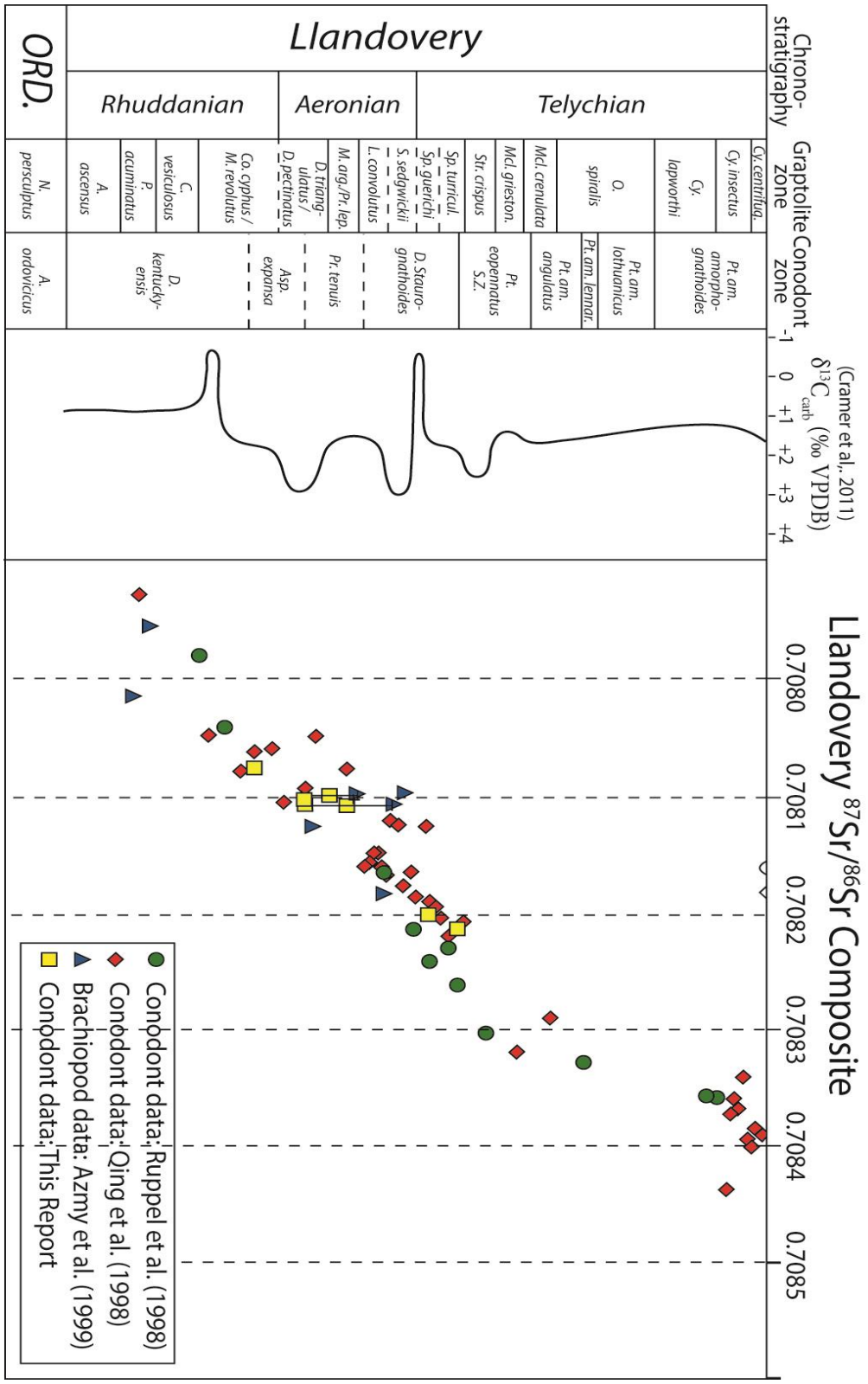

Figure 16: Composite $^{87}S/^{86}Sr$ for the Llandovery.

The deep-water environment in the basin-center position (Fig. 14) is represented in the Johnson #1-6, Freudenburg #1-31 and Sun-Bradley #4 cores. The ages of the Cabot Head Shale, the UD-BBG, and the Manistique Group in the basin-center are not constrained biostratigraphically. The $\delta^{13}C_{carb}$ curve of the Johnson #1-6 show 2 positive excursions (Fig. 13). The first (+2‰) starts in the middle section of the UD-BBG to the bottom of the core and the second (+3‰) occurs in the lower section of the Manistique Group. Based on an abrupt GR decrease at the contact between the Cabot Head Shale and the Lime Island (Fig. 7), the top of the Cabot Head Shale is identified at 8202 ft depth. Although the conodonts were collected from the Freudenburg #1-31 and $\delta^{13}C_{carb}$ data from the Johnson #1-6, the distance between the two wells is approximately 1 mile. This spatial proximity makes it likely that the lithology, age, and chemistry of the rocks are similar. This assumption is supported by very similar GR log signatures as well as a correlative elemental concentration trends of Al, K, Si, Ti, and Zr, that were measured in both of the wells using Portable Energy Dispersive X-ray Florescence (Al-Musawi and Kaczmarek 2018 a, b). The studied section in these wells is characterized by a distinctive low GR signature compared to the high GR signatures of the bounding units. Based on the $^{87}Sr/^{86}Sr$ (Fig. 16), the ages of these three samples were interpreted as Ae 1-Ae 2. As a result, first CIE 3‰ VPDB is defined as the Late Aeronian excursion (Ae 3; Cramer et al. 2011). The second CIE +2‰ is defined as the Early Aeronian excursion (Ae 1; Cramer et al. 2011). This suggests that age of the lower half of the UD-BBG in the basin-center is Ae 1, and the upper half of the UD-BBG and lower third of the Manistique Group is Ae 2.

4.3. Basin-wide Correlation

Prior studies by Harrison (1985), Kuglitsch (2000), and Voice et al. (2017) relied mostly on GR logs to identify and correlate lithologic units of the BBG in the subsurface across the Michigan Basin. The results of the current study add to this work by showing that the BBG was deposited at different times in different locations around the basin (Fig 15). The correlations presented here, which are based on conodont, $\delta^{13}C_{carb}$, and $^{87}Sr/^{86}Sr$ data, imply that the Cataract Group, BBG, and Manistique Group are older in the basin-center and become younger toward the shelf. For example, the upper section of the Cabot Head Shale, Lime Island, Byron, and lower section of the Hendricks at the shelf position are time equivalent to the upper section of the Byron,

Hendricks, and the lower section of the Schoolcraft in the slope position and the upper half of the UD-BBG and lower section of the Schoolcraft in the basin-center. The Byron and the Lime Island in the slope position is time equivalent to the lower half of the UD-BBG in the basin-center (Fig. 17). The upper section of the Hendricks in the shelf position is the time equivalent to the lower half of the Schoolcraft in the slope position and of the Schoolcraft in the basin-center (Fig. 17). These results indicate that the existing lithostratigraphic correlations between the three formations of the BBG in the north and the UD-BBG in the south are incorrect as only the Lime Island and Byron are time equivalent to the upper half of the UD-BBG in the basin-center.

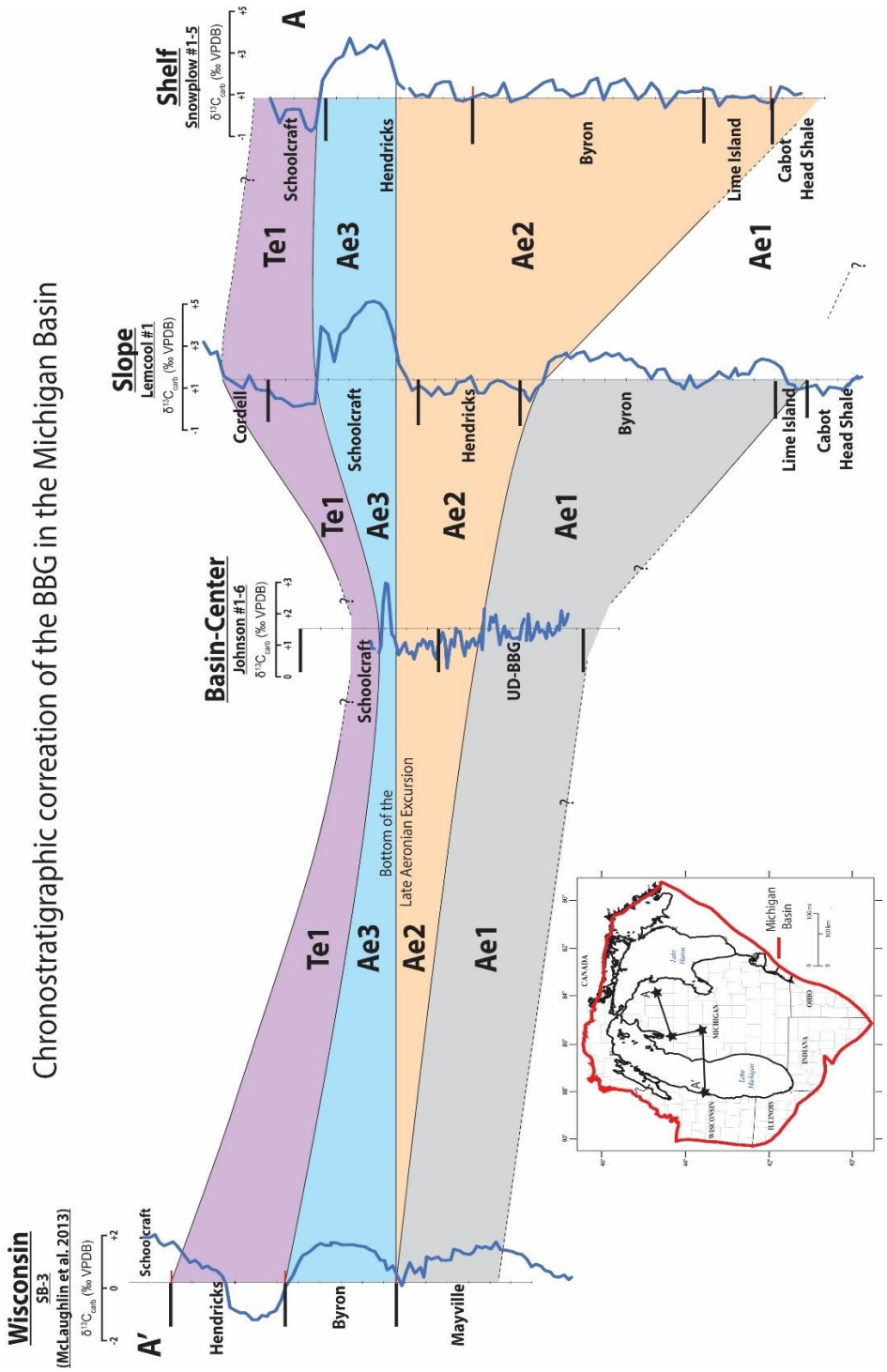

Figure 17: Proposed chronostratigraphic correlation of the BBG in the Michigan Basin, Bottom of the Late Aeronian Excursion is used as datum..

4.4. Michigan Basin Development during BBG Deposition

Given that the BBG has deposited at different times in different locations around the Michigan Basin, it is now possible, utilizing the new age data of this study, to correlate chronostratigraphic time correlative rock packages across the Michigan Basin. This framework will help to understand how the basin evolved during the Early Silurian. Based on the gradual thickness change of the BBG from north to the south, the BBG was previously interpreted to represent a broad carbonate ramp (Harrison 1985; Kuglitsch 2000; Voice et al. 2017). However, these studies used GR and facies descriptions to correlate the BBG assuming that the BBG's three formations in the north are time equivalent of the UD-BBG in the south. Applying the new findings from the current study suggests that the Middle Aeronian (Ae2) interval exhibits a drastic change in thickness between the shelf (~200 ft) and the slope (70 ft), whereas the Late Aeronian (Ae3) interval show similar thicknesses in both the shelf and the slope (Fig. 17). Therefore, these new findings suggest that the BBG was deposited on a carbonate rimmed shelf that changed sometime around the Ae3 to a carbonate ramp. This interpretation is further supported by deeper water facies identified within the Byron in the Ford and Scheuner Unit core located ~25 mi northeast the Snowplow #1-5 (appendix B).

Basin on the finding that the Middle Aeronian, Ae2, interval in the shelf position is comprised of the upper section of the Cabot Head Shale, Lime Island, Byron, and the lower section of the Hendricks (Fig. 17). In general, there are six major shallowing upward cycles in the Ae2 interval that were correlated from the shelf to the slope (Fig. 18). Also, there are number of the storm deposit layers that were identified within the Lime Island at the shelf position, the Hendricks at the slope position, and the upper part of the UD-BBG in basin-center position (Voice et al. 2017). The age data in the current study show that these storm deposit layers occur within the lower section of the Middle Aeronian interval in all three positions within the Michigan Basin. In separate studies by Al-Musawi and Kaczmarek (2018a,b) these storm deposit layers were identified and correlated across the basin using elemental variations as measured by ED-XRF. They showed that these layers tend to have higher concentration of Al, K, Si, Ti, and Zr, in shelf, slope, and basin-center positions (Al-Musawi and Kaczmarek 2018a, b) which they interpreted to reflect higher influx of continental materials. Except for the storm deposit layers, shallowing

upward depositional cycles cannot be recognized within the UD-BBG in the basin-center. More investigations are required to verify if these changes in sea level can be identified in the basin-center deposits.

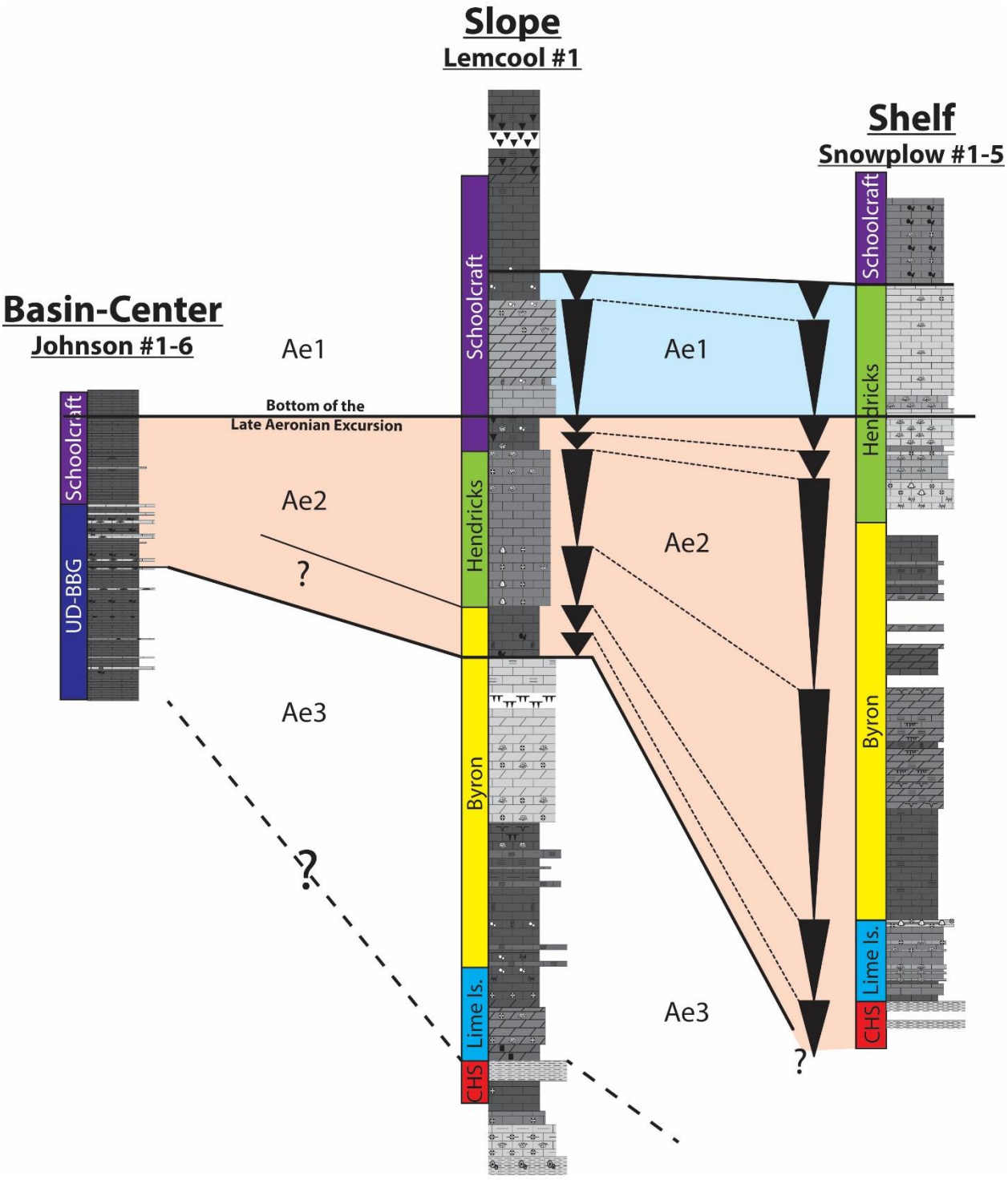

Figure 18: Proposed correlation of depositional cycles in the BBG from the shelf to the basin-center.

4.5. Correlating from Northwest Michigan to Northeast Wisconsin

Previous studies by Ehlers 1957 and Kuglitsch (2000) correlated the top of the Mayville, Byron, and the Hendricks formation of Wisconsin to the Lime Island, Byron and Hendricks formations of Michigan, respectfully. However, correlation between the $\delta^{13}C_{carb}$ curves of the Michigan Basin (this study) and the $\delta^{13}C_{carb}$ curve of northeast Wisconsin (McLoughlin et al. 2013) are inconsistent with one another. Based on the $\delta^{13}C_{carb}$ curve, the Early Aeronian excursion was recognized within the Byron in the slope, lower section of the UD-BBG in the basin-center, and the Mayville in Wisconsin, therefore, it was concluded that these three units are time equivalent (Fig. 17). The Lime Island, Byron, and the lower section of the Hendricks in the shelf position are characterized by a flat $\delta^{13}C_{carb}$ curve that is topped by a positive excursion (+3‰; Late Aeronian) (Fig. 17). This flat $\delta^{13}C_{carb}$ interval is missing in the Wisconsin $\delta^{13}C_{carb}$ curve. Therefore, it is more likely that the Lime Island, Byron, and the lower section of the Hendricks in the shelf position are time equivalent to an unconformity recognized by McLaughlin et al. (2013) in the Wisconsin section. The positive excursion (Late Aeronian CIE) that was recognized in the upper section of the Hendricks in the shelf, lower section of the Schoolcraft in the slope, upper section of the Schoolcraft in basin-center, and the Byron in Wisconsin suggests that these units are time equivalent. The negative shift in the $\delta^{13}C_{carb}$ curve overlies the Late Aeronian excursion that was recognized in the lower section of the Schoolcraft in the shelf, upper section of the Schoolcraft in the slope, and the lower section of the Hendricks in Wisconsin identifying these units are time equivalents (Fig. 17). This correlation suggests that the elevation of the northwest side of the Michigan Basin was most likely higher than the northeast side during the Middle Aeronian. As a result, the Middle Aeronian interval is completely missing in the Wisconsin, which could be a result of a higher subsidence rate in the northeast.

4.6. The Llandovery in Michigan Basin Compared to Other Basins

The $\delta^{13}C_{carb}$ curve for the Llandovery age has been described in many studies around the world (Kaljo and Martma 2000; Kaljo et al. 2003; Poldvere 2003; Melchin and Holmden 2006; Munnecke and Mannik 2009; Mclaughlin et al. 2013; Waid et al. 2017; McAdam et al. 2017: Mclaughlin et al. 2019). However, complete curves for the Llandovery age were constructed only in the Anticosti Island, Quebec, Canada (Braun 2018) and The Moose River Basin in Ontario,

Canada (Bancroft et al. 2015). The Llandovery is considered as a time of recovery after the latest Ordovician global sea level fall (Kaljo and Martma 2000). The climate during the Llandovery is interpreted as a greenhouse period that is interrupted by three glaciation episodes (Caputo 1998). As a result, most basins around the world were potentially exposed and experienced non-deposition and erosion during glacio-eustatic sea level falls. In contrast, the complete Llandovery rock section is well preserved in the Michigan Basin. This suggest that the Michigan Basin was deep enough to avid exposure during these global sea level falls and was still connected to the global ocean. Furthermore, studies that investigated the upper stratigraphic section of the Silurian in the Michigan Basin demonstrate the presence of the Ireviken, Mulde I, Mulde II, and the Lau excursions (Caruthers et al. 2018; Rine et al. in review). The Michigan Basin is one of the few locations around the world that have the entire Llandovery lithostratigraphic section preserved which gives researchers an opportunity to more fully understand the paleoclimate, the paleogeography, and the paleoenvironment during that geologic time.

Chapter 5
Conclusions

This study demonstrates the effectiveness of integrating multiple geological datasets to solve outstanding stratigraphic questions. More specifically, carbon isotope excursions, strontium isotopes, and conodont biostratigraphy were used to establish a chronostratigraphically correlation of the Burnt Bluff Group carbonates of the Michigan Basin from the shallow shelf to the deep basin. A number of carbon isotope excursions (CIEs) were identified in the BBG. These CIEs were age constrained using conodonts and strontium isotope ratios, and could be correlated to globally recognized events. The seven conodont samples that were analyzed for the $^{87}Sr/^{86}Sr$ in this study showed a promising result when compared to the global data set. Silurian conodonts with no biostratigraphic importance yield useful $^{87}Sr/^{86}Sr$ values used to further constrain ages.

One positive CIE was identified in the shelf position and was dated to the Late Aeronian. Three positive CIEs were identified in the slope position and were dated to the Early Aeronian, Late Aeronian, and Valgu. Two positive CIEs were identified in the basin-center position and were dated to the Early Aeronian and Late Aeronian. The presence of the three global carbon isotopes excursions (the Early Aeronian, the Late Aeronian, and the Valgu) of the Llandovery age in the Michigan Basin rock record demonstrates that the Michigan Basin is one of the few places around the world that has full section of the Llandovery preserved.

Based on the chronostratigraphic correlation between the shelf, the slope, and the basin-center, the BBG was deposited at different times in the different locations around the Michigan Basin. In general, the BBG is older toward the basin-center. Chronostratigraphically, the upper section of the Cabot Head Shale, Lime Island, Byron, and lower section of the Hendricks in the shelf are time equivalent to the upper section of the Byron, Hendricks, and the lower section of the Schoolcraft in the slope position. These same units, in contrast, are time equivalent to the upper half of the UD-BBG and lower section of the Schoolcraft in the basin-center. The Byron and the Lime Island in the slope position is time equivalent of the lower half of the UD-BBG in the

basin-center. The upper part of the Hendricks in the shelf position is the time equivalent of the lower half of the Schoolcraft in the slope position and of the Schoolcraft in the basin-center.

The chronostratigraphic correlation from the northeast (shelf) to the northwest (Wisconsin) lithostratigraphic sections of the Michigan Basin suggests the following: (i) The Byron in the slope position and the lower section of the UD-BBG in the basin-center correlate to the Mayville Formation in Wisconsin, (ii) The Lime Island, Byron, and Hendricks in the shelf, the Hendricks in the slope, and the upper section of the UD-BBG and lower section of the Schoolcraft in basin-center correlate to an unconformity in Wisconsin. (iii) The upper section of the Hendricks in the shelf, lower section of the Schoolcraft in the slope, and the upper section of the Schoolcraft in basin-center are time equivalents to the Byron in Wisconsin. (iv) The lower section of the Schoolcraft in the shelf position and the upper section of the Schoolcraft in the slope position are time equivalent to the Hendricks in Wisconsin.

Lastly, previous studies suggested that the BBG was deposited on broad carbonate ramp. However, the lithostratigraphic correlation using the new age data suggest that the BBG, during the Middle Aeronian, was deposited on carbonate rimmed shelf.

References

Ahm, A. S. C., Bjerrum, C. J., Blättler, C. L., Swart, P. K., & Higgins, J. A. (2018). Quantifying early marine diagenesis in shallow-water carbonate sediments. *Geochimica et Cosmochimica Acta*, 236, 140-159.

Al-Musawi, M., and Kaczmarek, S.E. (2018a) An integrated shelf to basin chemo- and chrono-stratigraphic correlation of the Burnt Bluff Group (BBG) carbonates, Michigan Basin, U.S.A (oral), *Geological Society of America Annual Meeting, Nov. 4-7, Indianapolis, IN, #323425 (74-2).*

Al-Musawi, M. and Kaczmarek, S.E. (2018b) Application of XRF, biostratigraphic, and carbon isotope data to establish a sequence stratigraphic framework and depositional facies model for the Burnt Bluff Group, Michigan Basin, USA (poster), American Association of Petroleum Geologists Annual Conference, May 20-23, Salt lake City, UT, #2855260.

Azmy, K., Veizer, J., Bassett, M. G., and Copper, P. (1998). Oxygen and carbon isotopic composition of Silurian brachiopods: implications for coeval seawater and glaciations. *Geological Society of America Bulletin*, *110*(11), 1499-1512

Barnes, D. A., Harrison III, W. B., and Wahr, A. (2009). Assessment of regional geological carbon sequestration potential in Upper Silurian to Middle Devonian strata of the Michigan Basin. *In* M. Grove, J. C. Pashin, and R. L. Dodge, (eds.), Carbon Dioxide Sequestration in geological media – State of the Science: AAPG Studies in Geology v. 59, p. 99-123.

Braun, M. (2018). *High Resolution Chemostratigraphy and Cyclostratigraphy of Lower Silurian Neritic Carbonates from Anticosti Island, Quebec, Canada*. Unpublished Doctoral dissertation, Université d'Ottawa/University of Ottawa).

Caruthers, A. H., Gröcke, D. R., Kaczmarek, S. E., Rine, M. J., Kuglitsch, J., & Harrison III, W. B. (2018). Utility of organic carbon isotope data from the Salina Group halite (Michigan Basin): A new tool for stratigraphic correlation and paleoclimate proxy resource. *Geological Society of America, Bulletin,* 130(11-12), 1782-1790.

Catacosinos, P. A. (1973). Cambrian lithostratigraphy of Michigan basin. *AAPG Bulletin*, *57*(12), 2404-2418.

Catacosinos, P. A., Daniels Jr, P. A., and Harrison III, W. B. (1990). Structure, Stratigraphy, and Petroleum Geology of the Michigan Basin: Chapter 30, *In* M. W. Leighton, D. R. Kolata, D. T. Oltz, and J. J. Eidel (eds.), Interior Cratonic Basins, AAPG Memoir, v. 51, p. 561-601.

Catacosinos, P. A., Harrison, W. B., III, Reynolds, R. F., Westjohn, D. B., and Wollensak, M. S. (2001). *Stratigraphic lexicon for Michigan*. Michigan Geological Survey Division Bulletin, v. 8, 56 p.

Chamberlin, T. C. (1877). Geology of eastern Wisconsin. *Geology of Wisconsin*, *2*(part 2), 268-287.

Chen, Z., Männik, P., and Fan, J. (2017). Llandovery (Silurian) conodont provincialism: An update based on quantitative analysis. *Palaeogeography, Palaeoclimatology, Palaeoecology*, *485*, 661-672.

Cramer, B. D., and Saltzman, M. R. (2005). Sequestration of ^{12}C in the deep ocean during the early Wenlock (Silurian) positive carbon isotope excursion. *Palaeogeography, Palaeoclimatology, Palaeoecology*, *219*(3-4), 333-349.

Cramer, B. D., Brett, C. E., Melchin, M. J., Maennik, P., Kleffner, M. A., McLaughlin, P. I., ... and Brunton, F. R. (2011). Revised correlation of Silurian Provincial Series of North America with global and regional chronostratigraphic units and $\delta^{13}C_{carb}$ chemostratigraphy. *Lethaia*, *44*(2), 185-202.

Cramer, B. D., Munnecke, A., Schofield, D. I., Haase, K. M., and Haase-Schramm, A. (2011). A revised $^{87}Sr/^{86}Sr$ curve for the Silurian: Implications for global ocean chemistry and the Silurian timescale. *The Journal of Geology*, *119*(4), 335-349.

Ehlers, G. H. (1921). Niagaran rocks of the Northern Peninsula of Michigan: Geol. Soc. *America Bull*, *32*, 129-130.

Ehlers, G. M., and Kesling, R. V. (1957). Silurian rocks of the northern peninsula of Michigan: Michigan Basin Geological Society, 62 p.

Ells, G. D. (1962). Silurian rocks in the subsurface of southern Michigan. *Silurian Rocks of the Southern Lake Michigan Area Michigan Basin Geological Society Annual Field Conference*, 39-49.

Friedman, G. M., and Kopaska-Merkel, D. C. (1991). Late Silurian pinnacle reefs of the Michigan Basin, In Catacosinos, P. A., and Daniels, P. A. (eds.), Early Sedimentary Evolution of the Michigan Basin, *Geological Society of America, Special Paper*, *256*, p. 89-100.

Grammer, G. M., Noack, A., Qualman, H., Ritter-Varga, A., Wold, J., Sandomierski, A., and Harrison III, W. B. (2010). Reservoir characterization of Silurian (Niagaran) “pinnacle” reefs in the Michigan Basin. *Search and Discovery Article*, *50286* posted July 30, 2010. Document

adapted from oral presentation at AAPG Annual Convention and Exhibition, New Orleans, LA: April 11-14, 2010.

Harrison III, W. B., Cercone, K. R., and Budai, J. M. (1985). Lithofacies and depositional environments of the Burnt Bluff Group in the Michigan basin. *Ordovician and Silurian rocks of the Michigan basin and its margins: Michigan Basin Geological Society Special Paper*, *4*, 95-108.

Howell, P. D., and Van Der Pluijm, B. A. (1999). Structural sequences and styles of subsidence in the Michigan basin. *Geological Society of America Bulletin*, *111*(7), 974-991.

Johnson, M. E., and Campbell, G. T. (1980). Recurrent carbonate environments in the Lower Silurian of northern Michigan and their inter-regional correlation. *Journal of Paleontology*, 1041-1057.

Kaljo, D., and Martma, T. (2000, July). Carbon isotopic composition of Llandovery rocks (East Baltic Silurian) with environmental interpretation. In *Proceedings of the Estonian Academy of Sciences, Geology* (Vol. 49, No. 4, pp. 267-283).

Kaljo, D., Martma, T., Männik, P., and Viira, V. (2003). Implications of Gondwana glaciations in the Baltic late Ordovician and Silurian and a carbon isotopic test of environmental cyclicity. *Bulletin de la Société géologique de France*, *174*(1), 59-66.

Kuglitsch, J. J. (2000). Correlation of the Silurian rocks of southeastern and northeastern Wisconsin using conodonts and conodont strontium isotope ratios and proposed conodont and ostracode biofacies models for the environs of the middle Aeronian Michigan Basin. Unpublished PhD Dissertation, University of Wisconsin, Madison, 349 p.

Kump, L. R., and Arthur, M. A. (1999). Interpreting carbon-isotope excursions: carbonates and organic matter. *Chemical Geology*, *161*(1-3), 181-198.

Loydell, D. K. (2007). Early Silurian positive $\delta^{13}C$ excursions and their relationship to glaciations, sea-level changes and extinction events. *Geological Journal*, *42*(5), 531-546.

McArthur, J. M. (1994). Recent trends in strontium isotope stratigraphy. *Terra Nova*, *6*(4), 331-358.

McAdams, N. E., Bancroft, A. M., Cramer, B. D., and Witzke, B. J. (2017). Integrated carbon isotope and conodont biochemostratigraphy of the Silurian (Aeronian–Telychian) of the East-Central Iowa Basin, Iowa, USA. *Newsletters on Stratigraphy*, *50*(4), 391-416.

McLaughlin, P. I., Mikulic, D. G., and Kluessendorf, J. (2013). Age and correlation of Silurian rocks in Sheboygan, Wisconsin, using integrated stable carbon isotope stratigraphy and facies analysis. *Geoscience Wisconsin*, *21*, 15-38.

Melchin, M. J., and Holmden, C. (2006). Carbon isotope chemostratigraphy in Arctic Canada: sea-level forcing of carbonate platform weathering and implications for Hirnantian global correlation. *Palaeogeography, Palaeoclimatology, Palaeoecology*, *234*(2-4), 186-200.

Munnecke, A., and Männik, P. (2009). New biostratigraphic and chemostratigraphic data from the Chicotte Formation (Llandovery, Anticosti Island, Laurentia) compared with the Viki core (Estonia, Baltica). *Estonian Journal of Earth Sciences*, *58*(3).

Palmer, M. R. (1992). Controls over the chloride concentration of submarine hydrothermal vent fluids: evidence from Sr/Ca and $^{87}Sr/^{86}Sr$ ratios. *Earth and Planetary Science Letters*, *109*(1-2), 37-46.

Patterson, W. P., and Walter, L. M. (1994). Depletion of ^{13}C in seawater $\Sigma C0_2$ on modern carbonate platforms: Significance for the carbon isotopic record of carbonates. *Geology*, *22*(10), 885-888.

Pollock, C. A., Rexroad, C. B., and Nicoll, R. S. (1970). Lower Silurian conodonts from northern Michigan and Ontario. *Journal of Paleontology*, 44, 743-764.

Rine, M., Garrett, J., and Kaczmarek, S. E. (2017). A new facies architecture model for the Silurian Niagara–Lower Salina "pinnacle" reef complexes of the Michigan Basin. In A. J. McNeill, J. Lonnee, and R. Wood (eds.). *Characterization and Modeling of Carbonates—Mountjoy Symposium* (Vol. 1), Society for Sedimentary Geology, SEPM Special Publication 109, p. 70-86.

Ruppel, S. C., James, E. W., Barrick, J. E., Nowlan, G. O. D. F. R. E. Y., Uyeno, T. T., Landing, E., & Johnson, M. E. (1998). High-resolution Silurian 87Sr/86Sr record: evidence of eustatic control of seawater chemistry. *Silurian cycles: linkages of dynamic stratigraphy with atmospheric, oceanic, and tectonic changes. New York State Museum Bulletin*, 491, 285-295.

Saltzman, M. R., Edwards, C. T., Leslie, S. A., Dwyer, G. S., Bauer, J. A., Repetski, J. E., ... & Bergström, S. M. (2014). Calibration of a conodont apatite-based Ordovician 87Sr/86Sr curve to biostratigraphy and geochronology: Implications for stratigraphic resolution. *Geological Society of America Bulletin*, 126(11-12), 1551-1568.

Sears, S. O., and Lucia, F. J. (1979). Reef-growth model for Silurian pinnacle reefs, northern Michigan reef trend. *Geology*, *7*(6), 299-302.

Sleep, N. H., and Sloss, L. L. (1978). A deep borehole in the Michigan Basin. *Journal of Geophysical Research: Solid Earth*, *83*(B12), 5815-5819.

Smith, R. A. (1915). Limestones of Michigan: Michigan Geological and Biological Survey, Publ. 21, Geol. *Series*, *17*, 101-311.

Swartz, C. K., Alcock, F. J., Butts, C., Chadwick, G. H., Cumings, E. R., Decker, C. E., Ehlers, G. M., Foerste, A. F., Gillette, T., Kindle, E. M., Kirk, E., Northrop, S. A., Prouty, W. F., Savage, T. E., Shrock, R. R., Swartz, F. M., Twenhofel, W. H., and Williams, M. Y. (1942). Correlation of the Silurian formations of North America. *Bulletin of the Geological Society of America*, *53*(4), 533-538.

Veizer, J.; Ala, D.; Azmy, K.; Bruckschen, P.; Buhl, D.; Bruhn, F.; Carden, G. A. F., et al. 1999. $^{87}Sr/^{86}Sr$, $\delta^{13}C$ and $\delta^{18}O$ evolution of Phanerozoic seawater. *Chemical Geology*. 161:59–88.

Voice, P. J., Harrison III, W. B., and Grammer, G. M. (2018). A reevaluation of the Burnt Bluff Group (Llandovery, Silurian, Michigan Basin) from subsurface and outcrop data: Development of a time-transgressive depositional model. In G. M. Grammer, W. B. Harrison III, and D. A. Barnes (eds.). *Paleozoic Stratigraphy and Resources of the Michigan Basin*, Geological Society of America Special Paper v. *531*, p. 55-79.

Watkins, R., and Kuglitsch, J. J. (1997). Lower Silurian (Aeronian) megafaunal and conodont biofacies of the northwestern Michigan Basin. *Canadian Journal of Earth Sciences*, *34*(6), 753-764.

Zhang, S., and Barnes, C. R. (2002). A new Llandovery (early Silurian) conodont biozonation and conodonts from the Becscie, Merrimack, and Gun River formations, Anticosti Island, Québec. *Journal of Paleontology*, *76*(sp57), 1-47.

Appendix A: Facies Photos and Description of the BBG in the Michigan Basin.

The Cabot Head Shale, Lime Island, Byron, Hendricks and UD-BBG lithofacies and sedimentary structures that were identified in the Michigan Basin.

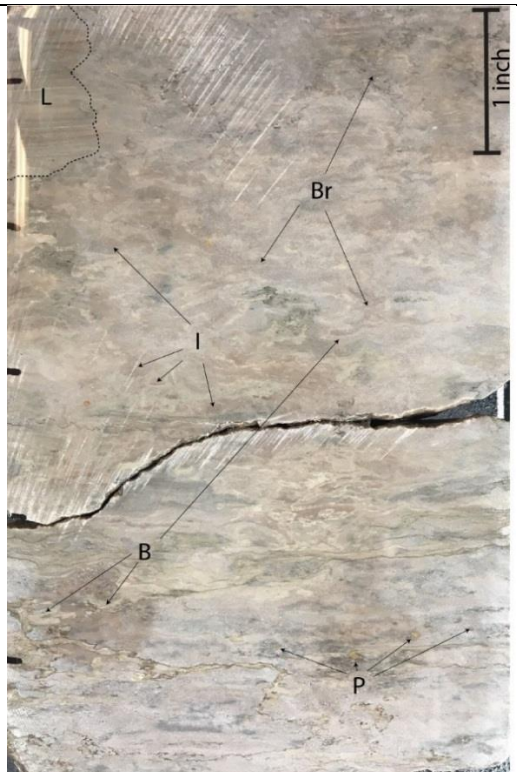

Figure 19: Facies 1, Cabot Head Shale, Snowplow #1-5, 5736.5ft, Br=Burrows, B= Brachiopods shell, I= Interaclasts, L= Lamination, P= Pyrite nodules.

Facies 1: Gray to dark gray laminated wackestone, composed of limestone. Intraclasts and abraded brachiopods shells are present in this facies. The lamination in this facies has been disturbed by heavy bioturbation and burrowing. Pyrite nodules are present in the lower section of this facies. Also, it is more argillaceous in the lower section.

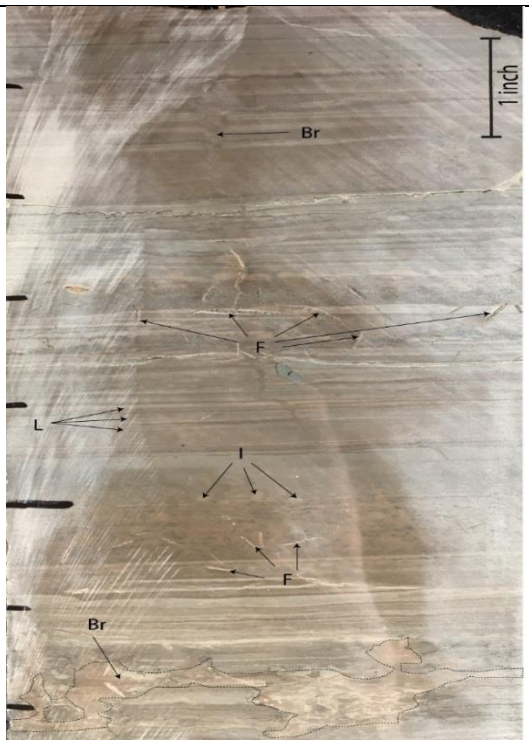

Figure 20: Facies 2, Cabot Head Shale, Snowplow #1-5, 5736ft, Br=Burrows, F= fenestrae, I= Interaclasts, L= Lamination

Facies 2: Gray to dark gray laminated mudstone, composed of limestone. Burrows are common in this facies. Small undefined interclass are present. Fenestral needles are common in this facies.

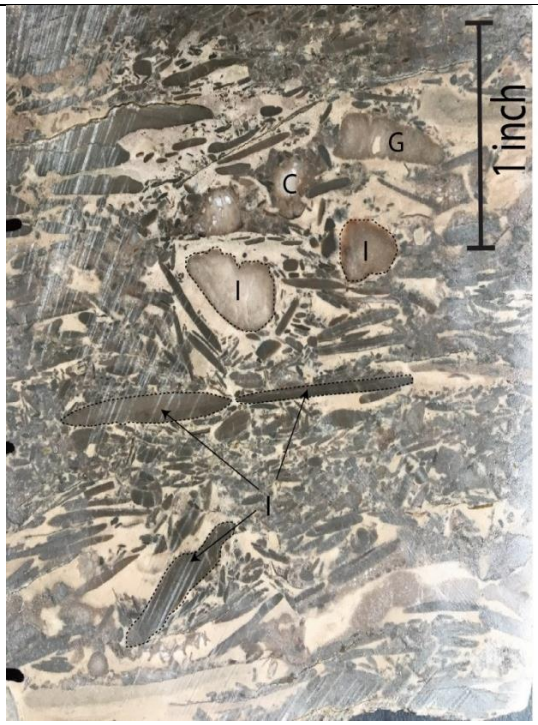

Figure 21: Facies 3, Bottom of the Lime Island Fm., Snowplow #1-5, 5734ft, C=corals, G= gastropods, I= Interaclasts

Facies 3: Light gray grain stone, composed of limestone (grains) and dolomite (matrix). The Interaclasts in this facies are very abundant. The orientation of the Interaclast are random, also the sizes of the grains varies between few millimeters to 3 cm. Some undefined fossils, corals pieces and abraded gastropods are present in this facies.

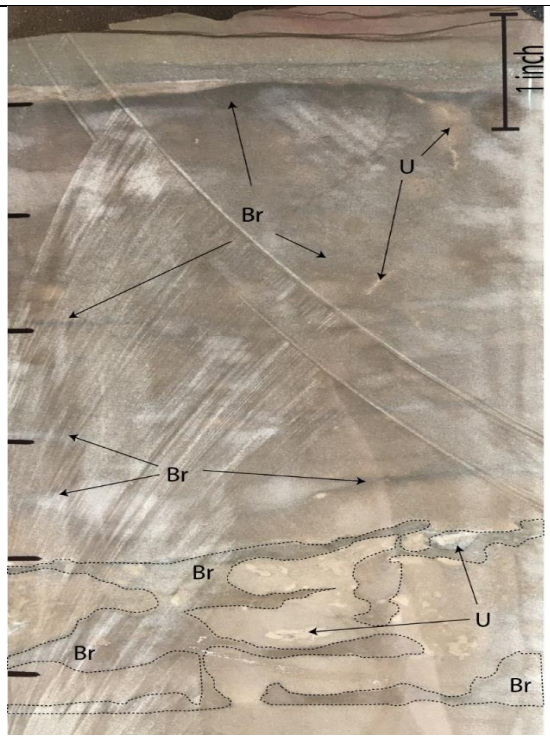

Figure 22: Facies 4, Bottom of the Lime Island Fm., Snowplow #1-5, 5733ft, Br=Burrows, U= Undefined

Facies 4: Light to dark gray burrowed mudstone, dolomitic limestone. This facies is heavily burrowed; the original texture is not preserved due to the burrowing. Some undefined fragments are present in this facies too.

Figure 23: Facies 5, Lime Island Fm, Snowplow #1-5, 5728ft, B= Brachiopods shell, I= Interaclasts

Facies 5: Light gray skeletal grain supported packstone, composed of limestone. The brachiopod shells are randomly oriented. Interaclast are situated between the brachiopod's shells.

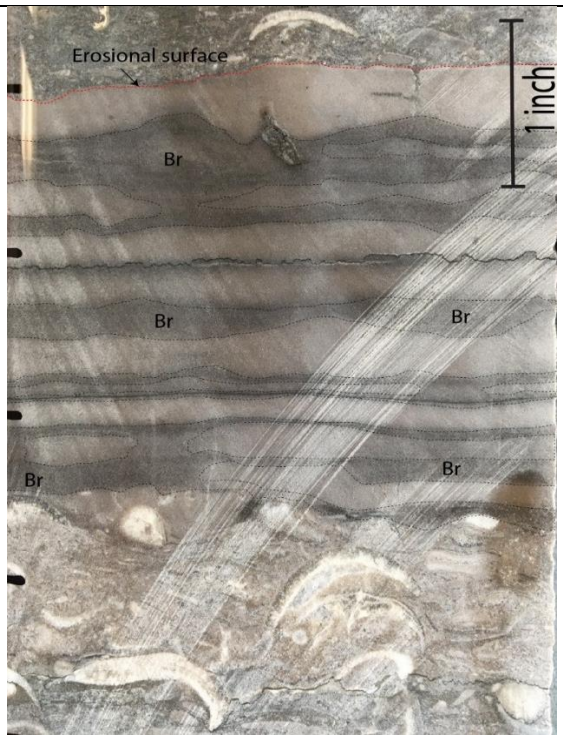

Figure 24: Facies 6, Lime Island Fm, Snowplow #1-5, 5730ft, Br=Burrows

Facies 6: Light to dark gray mudstone, composed of limestone. burrowed, sharp contacts with the overlying and underlying facies. There are no grains that can be seen with the naked eye. The upper contact is most likely representing an erosional surface.

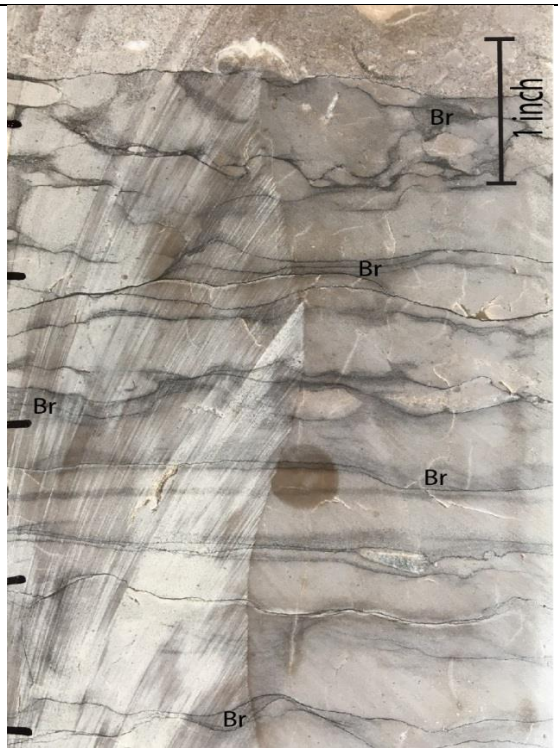

Figure 25: Facies 7, Lime Island Fm, Snowplow #1-5, 5724ft, Br=Burrows

Facies 7: Light gray to gray nodular mudstone, composed of limestone. Burrowed, the burrowing shape and orientation are different than the burrows in facies 6. There are some undifferentiated grains present in this facies.

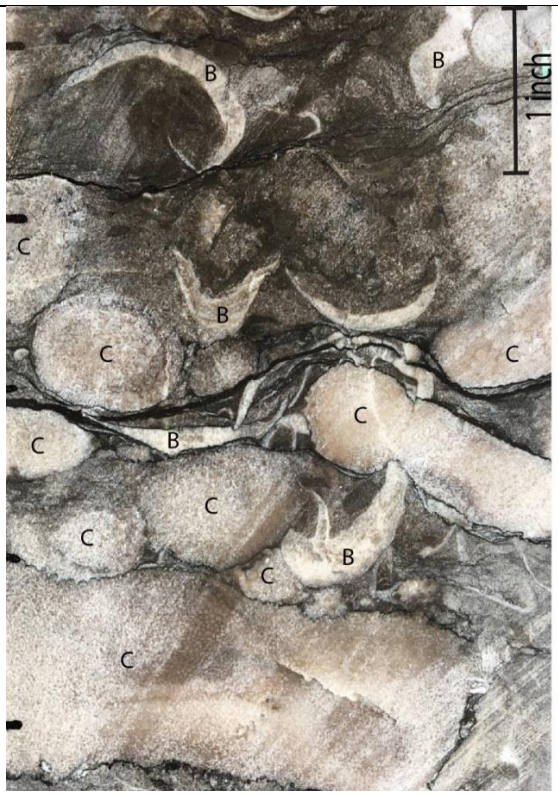

Figure 26: Facies 8, Lime Island Fm, Snowplow #1-5, 5710ft C=corals, B= brachiopods

Facies 8: Dark gray grain supported packstone, composed of limestone. Skeletal material is very abundant within this facies, mostly corals and brachiopods. There is now specific orientation to these corals and brachiopods shell. This facies has more corals and less brachiopods in the contrary of facies 5 that have more brachiopods and less corals.

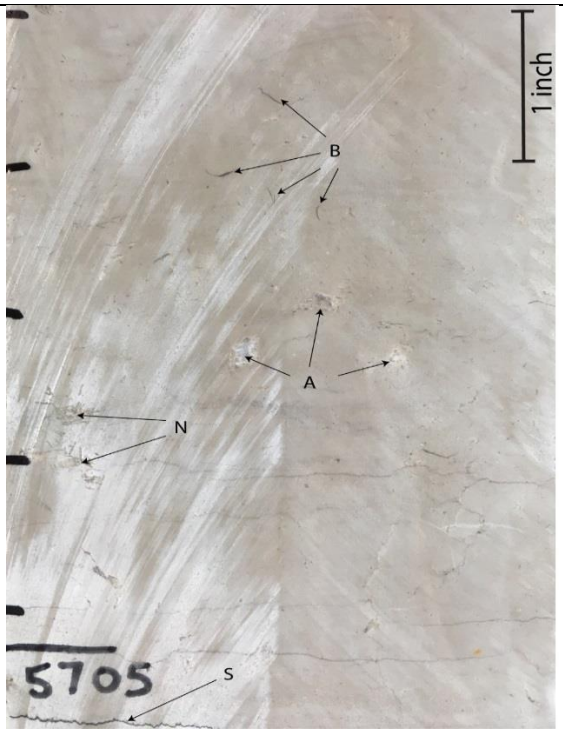

Figure 27: Facies 9, Byron Fm, Snowplow #1-5, 5705ft B= Brachiopods shell, A= Anhydrite nodules, N= Anhydrite needles, S= Stylolite

Facies 9: Light gray mudstone, dolomitic limestone. very small brachiopods shells are common in this facies, these shells have no orientation suggest that they have been transported. Anhydrite nodules and needles are common in this facies.

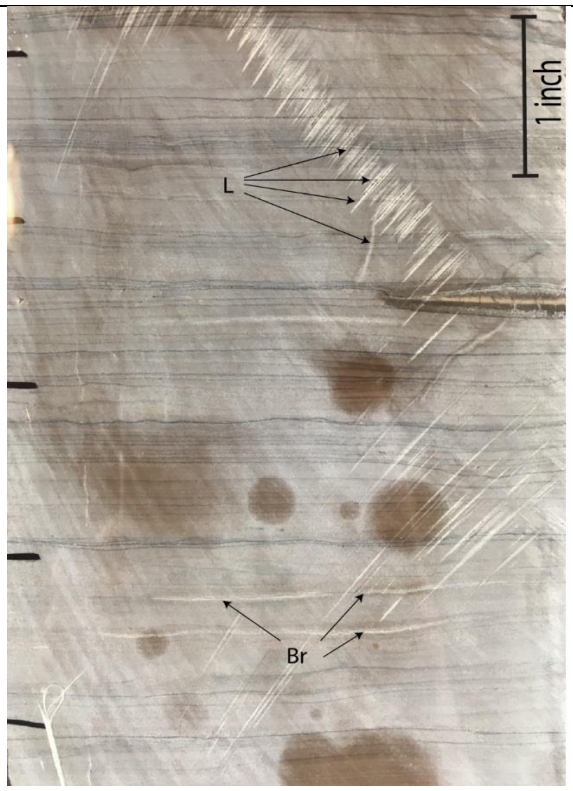

Figure 28: Facies 10, Byron Fm, Snowplow #1-5, 5704ft,Br= Burrows, L= Lamination

Facies 10: Dark to light gray, laminated mudstone. Horizontal burrows are present in this facies. It seems that some of the lamination is not due to bedding, but it is more likely to represent condensed stylolite due to overburden pressure.

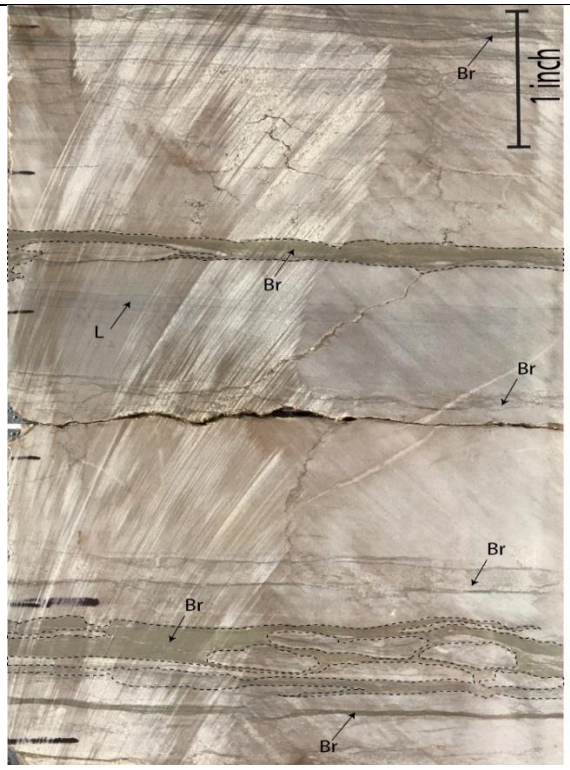

Figure 29: Facies 11, Byron Fm, Snowplow #1-5, 5695ft,Br= Burrows, L= Lamination

Facies 11: Dark gray laminated mudstone. Composed of limestone. Burrows are very abundant in this facies, the intensity and the size of the burrowing vary in this facies.

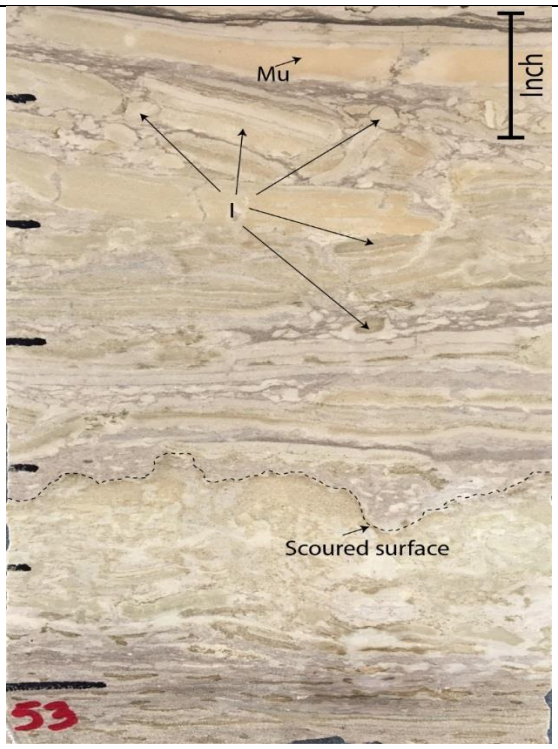

Figure 30: Facies 12, Byron Fm, Snowplow #1-5, 5653ft, Mu= Mudcrak, I= Interaclasts

Facies 12: Tan, Burrowed-mottled, Wackstone, laminated, horizontal burrowing, mud cracks common in this facies, rare skeletal grains of indeterminate origin, Interaclast up to 4cm in diameter are sub-angular to sub-rounded in outline.

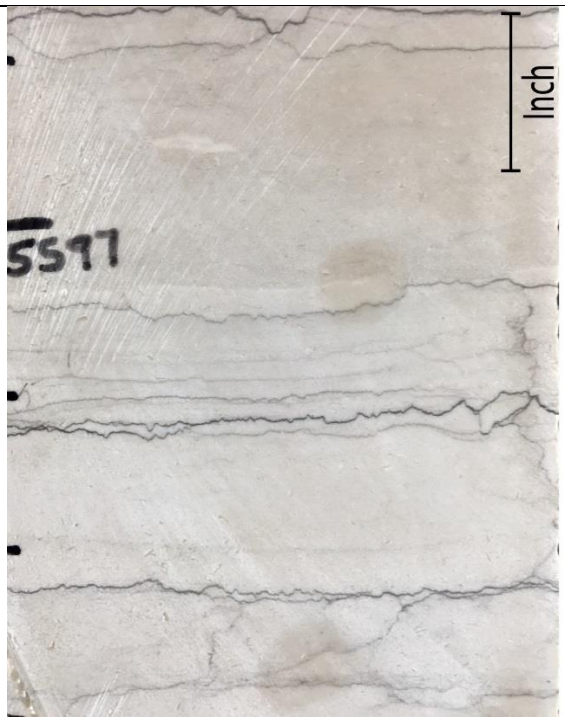

Figure 31: Facies 13, Hendricks Fm, Snowplow #1-5, 5597ft,

Facies 13: Light gray to tan colored, wispy-laminated, nodular fabric, heavy stylolitization.

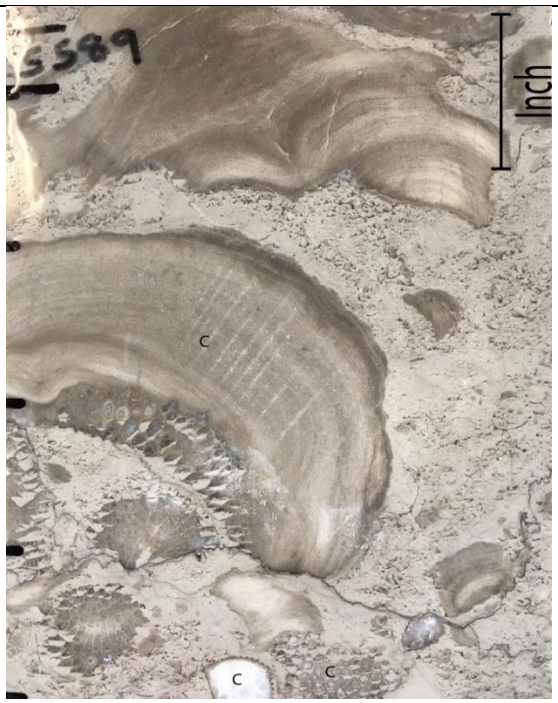

Figure 32: Facies 14, Hendricks Fm, Snowplow #1-5, 5589ft C= Corals

Facies 14: Light gray colored, skeletal packstone dominated by coral and Stromatoporoid.

Figure 33: Facies 15, UD-BBG, Johnson #1-6, 8186ft

Facies 15: Gray to dark gray, nodular burrowed mudstone.

Appendix B: Byron Fm. in the Ford and Scheuner Unit Core.

The contact between the Lime Island and Byron in the Ford and Scheuner Unit core. The picture also below shows the facies of the Byron formation. Based on the color, sedimentary structure, and the fossils content, facies of the Byron are interpreted to be deposited in deeper water environment than the facies of the Byron in the snowplow #1-5 core (Appendix F)

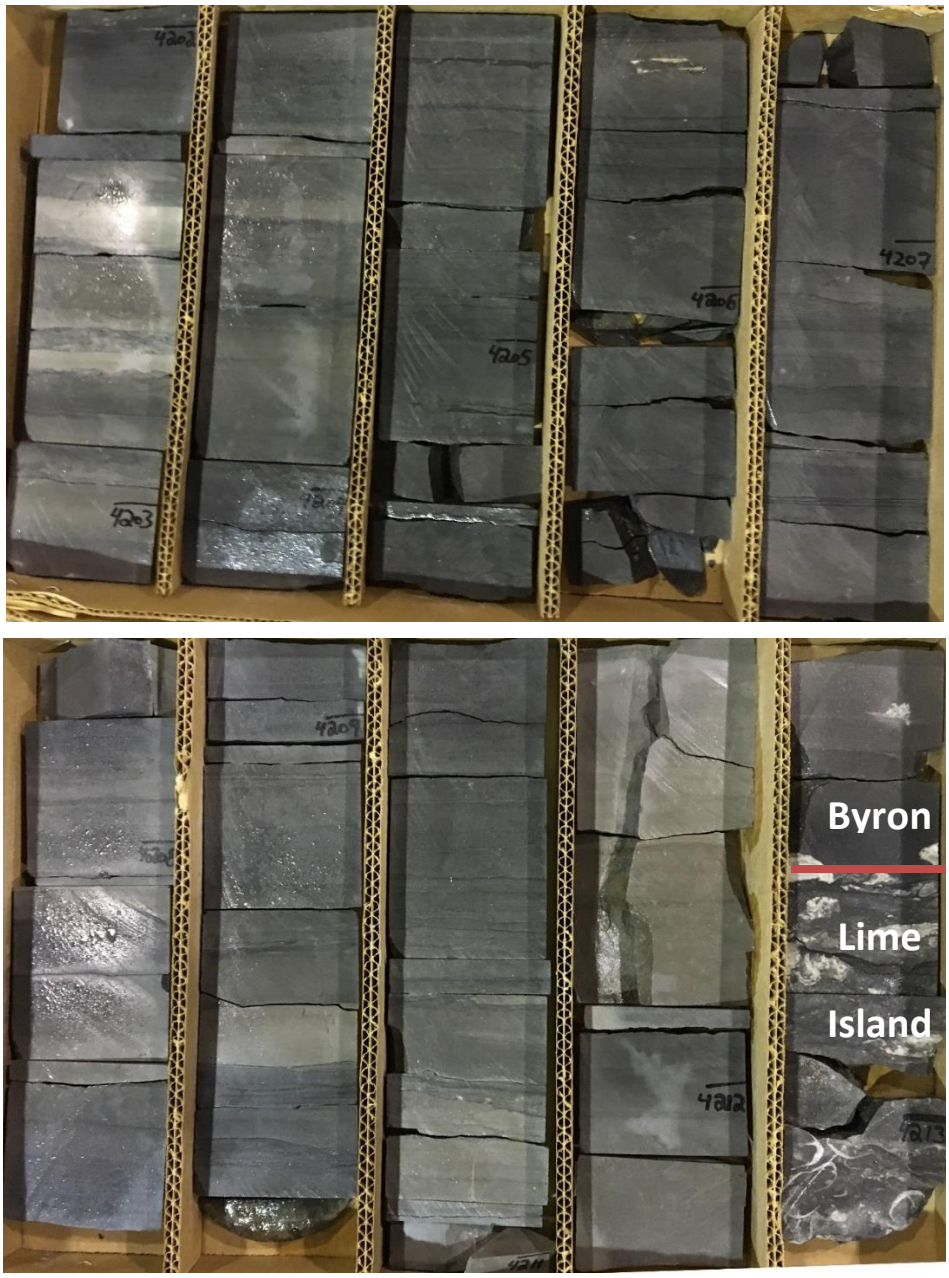

Figure 34: The Lime Island and Byron formations in the Ford and Scheuner Unit core, 4202-4213ft.

Appendix C: Cabot Head Shale Core Photos

Facies of the Cabot Head Shale in the Snowplow #1-5 and the Lemcool #1 cores and the contacts with the Lime Island.

Snowplow #1-5:

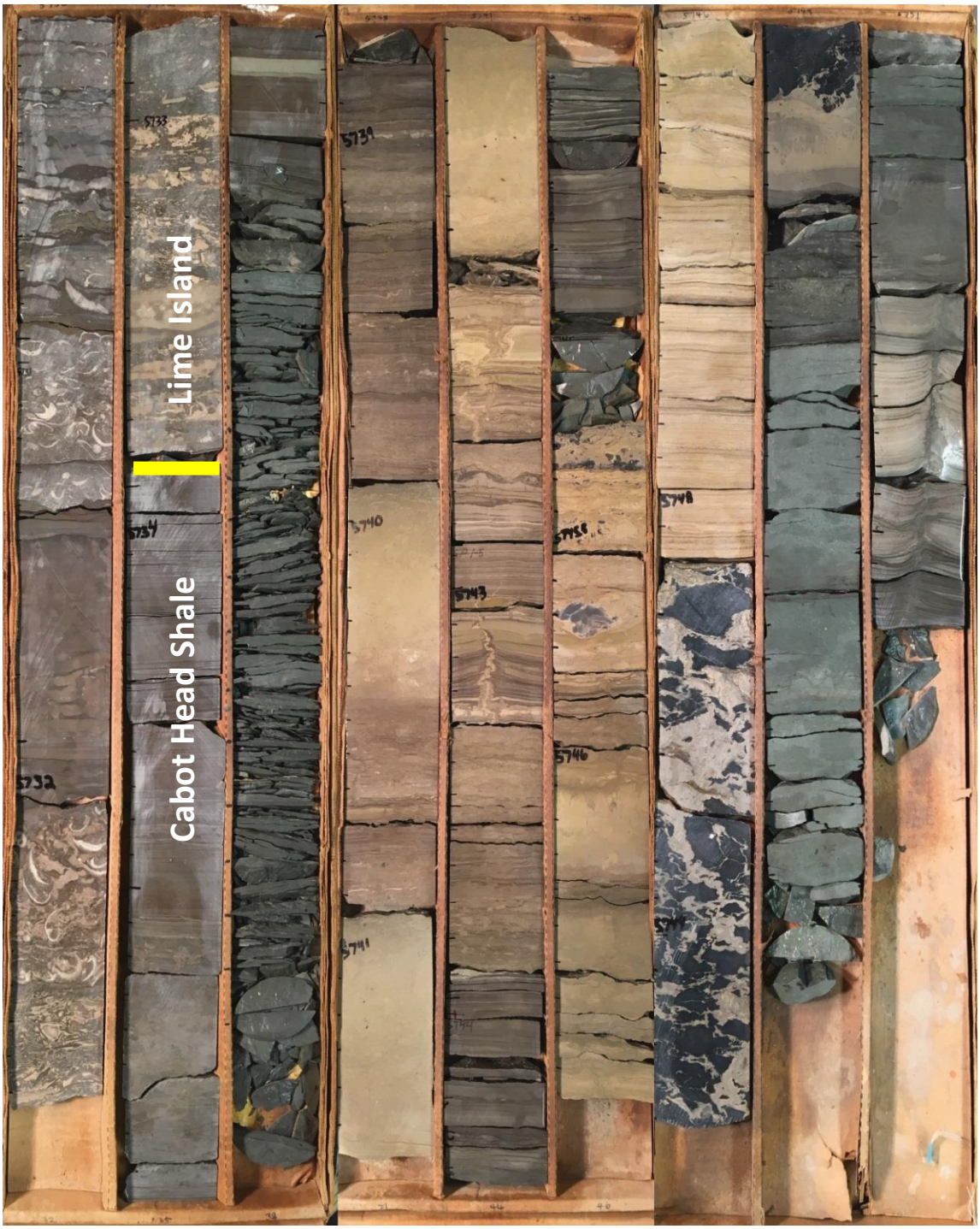

Figure 35: Cabot Head Shale and the lower section of the Lime Island Fm. in the Snowplow #1-5 core, 5730-5755ft

Lemcool #1:

Figure 36: The Cabot Head Shale and the lower section of the Lime Island Fm. in the Lemcool #1 core, 7236-7250ft.

Appendix D: Lime Island Fm. Core Photos

The lime Island in Snowplow #1-5 and the Lemcool #1

Snowplow #1-5:

Figure 37: The Contact between Lime Island and the Byron Fms. in the Snowplow #1-5 core, 5700-5721ft.

Figure 38: The contact between Lime Island and Cabot Head Shale in the Snowplow #1-5 core, 5722-5736ft.

Lemcool #1:

Figure 39: The Lime Island Fm. in the Lemcool #1 core, 7221-7235ft.

Figure 40: The contact between the Lime Island and Byron Fms. in the Lemcool #1 core, 7207-7220ft.

Appendix E: Byron Fm. Core Photos

Sections of the Byron in the Snowplow #1-5 and the Lemcool #1

Snowplow #1-5

Figure 41: The lower section of the Byron Fm. in the Snowplow #1-5 core, 5686-5707ft.

Figure 42: The Upper section of the Byron Fm. in the Snowplow #1-5 core, 5661-5686ft.

Lemcool #1:

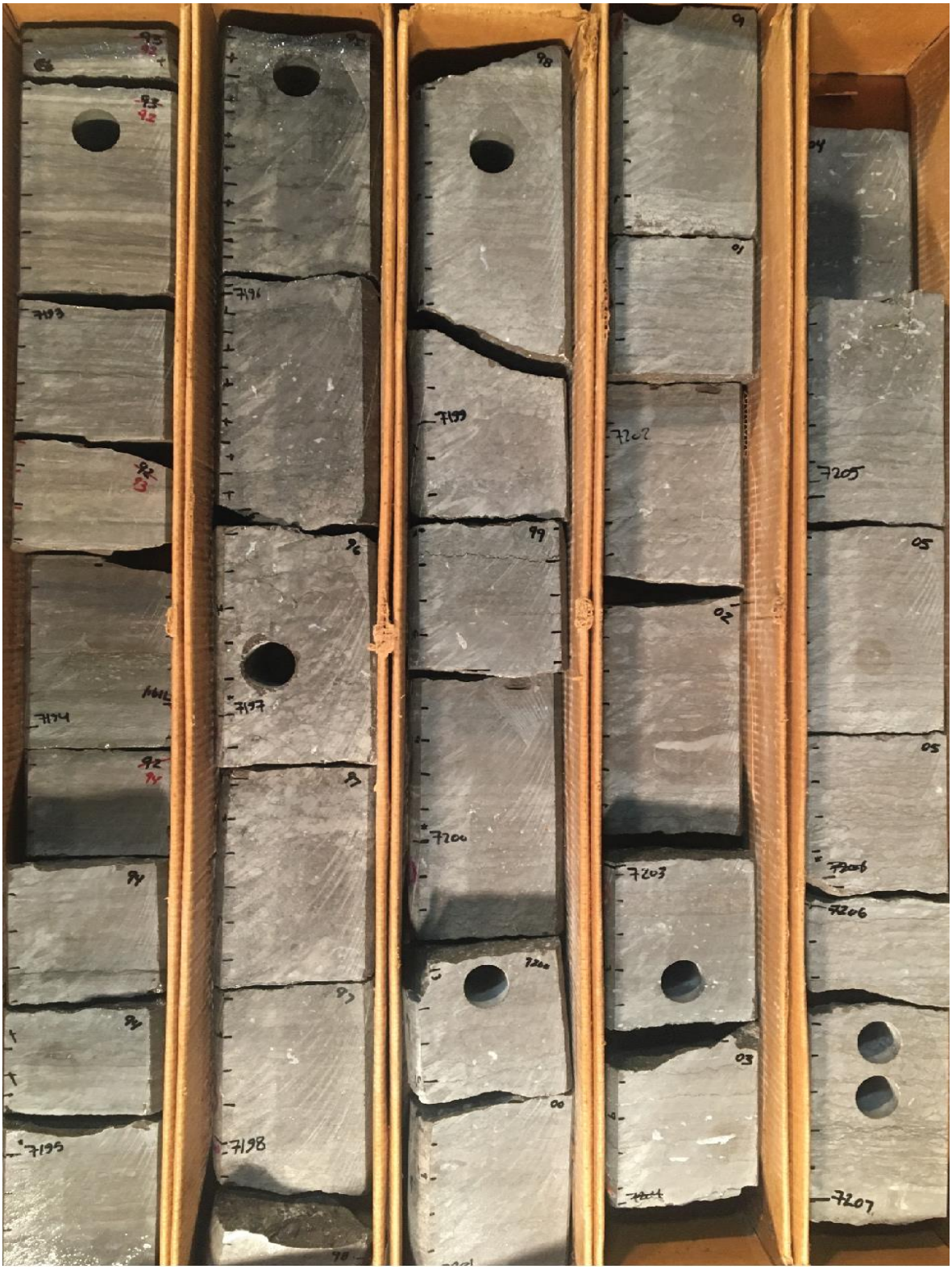

Figure 43: The lower section of the Byron Fm. in the Lemcool #1 core, 7192-7207ft.

Figure 44: The middle section of the Byron Fm. in the Lemcool #1 core, 7137-7150ft.

Appendix F: Hendricks Fm. Core Photos

Hendricks in the Snowplow #1-5 and the Lemcool #1

Snowplow #1-5

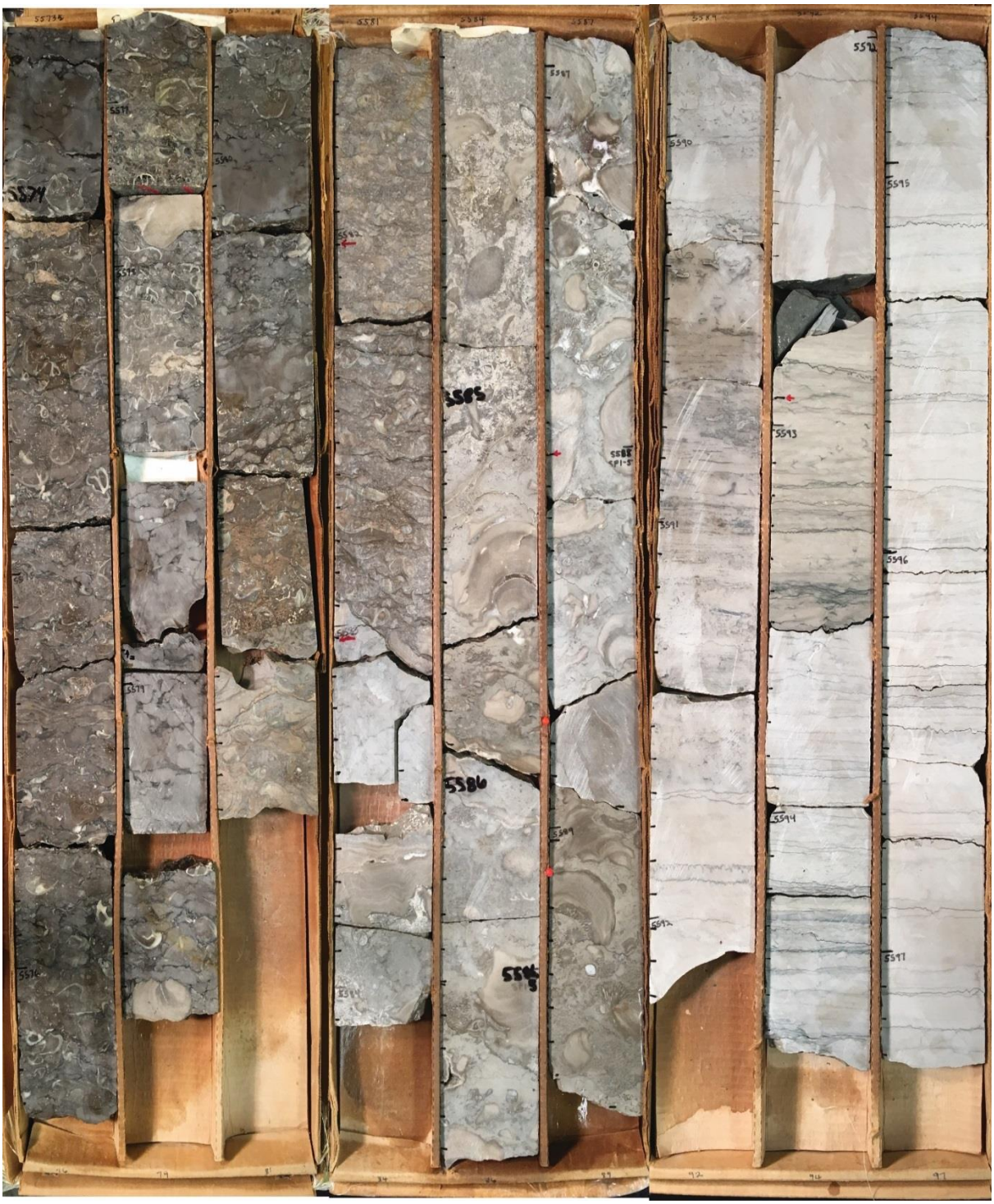

Figure 45: The Hendricks Fm. in the Snowplow #1-5 core, 5974-5597ft.

Lemcool #1

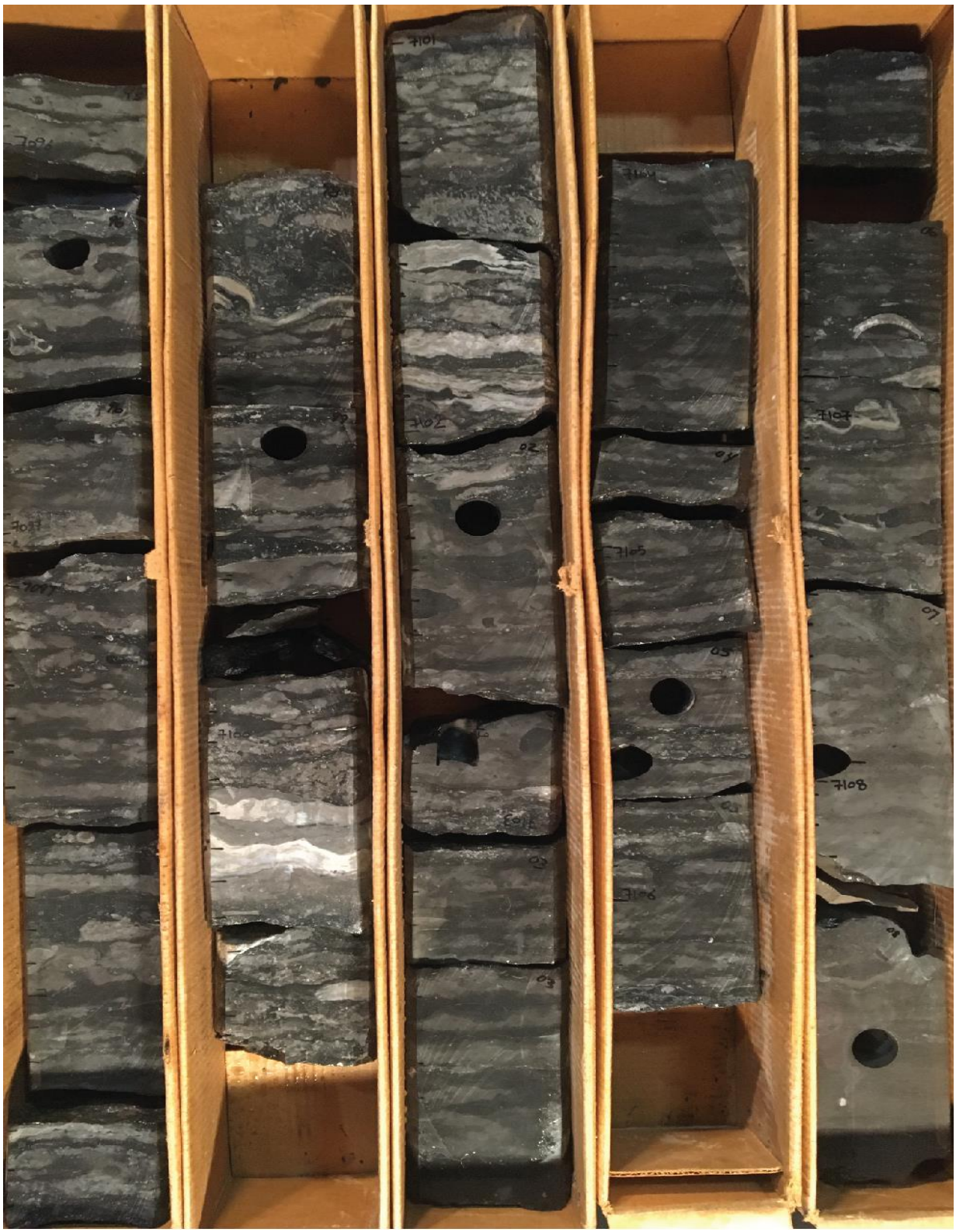

Figure 46: The lower section of the Hendricks Fm. in the Lemcool #1 core, 7094-7109ft.

Figure 47: The upper section of the Hendricks Fm. in the Lemcool #1 core, 7068-7081ft.

Appendix G: Carbon and Oxygen Isotopes data

Table 3: Carbon and Oxygen data results.

Lemcool #1		
Depth (ft)	**$\delta\ ^{13}C_{carb}$**	**$\delta\ ^{18}O_{carb}$**
6963	2.98	-7.91
6966	2.37	-6.39
6969	2.50	-6.08
6972	1.26	-7.75
6981	0.64	-6.65
6984	1.30	-5.56
6987	0.60	-5.59
6990	0.53	-5.51
6993	0.54	-6.06
6996	0.12	-5.79
6999	0.12	-5.31
7002	-0.10	-6.00
7004	-0.27	-5.60
7007.75	-0.23	-5.91
7011	-0.15	-6.29
7014	-0.14	-4.88
7017	3.75	-7.60
7020	3.38	-7.47
7023	2.01	-7.25
7026	3.38	-7.42
7029	3.71	-7.65
7032	4.26	-7.49
7035	4.59	-7.89
7038	4.99	-7.41
7041	5.07	-7.66
7044	4.94	-7.12
7047	4.56	-7.09
7050	3.45	-7.54
7053	1.85	-6.72
7056	1.25	-6.97
7059	0.56	-7.15
7062	0.79	-5.97
7065	0.56	-6.74
7068	0.26	-6.75
7071	0.70	-6.88
7074	0.34	-7.02
7077	0.42	-5.84
7080	0.96	-6.57

7083	1.02	-6.36
7086	1.24	-6.01
7089	0.40	-7.14
7092	0.40	-6.75
7095	0.89	-5.37
7098	1.03	-5.29
7101	0.99	-6.00
7104	0.76	-5.38
7107	0.62	-5.41
7110	0.54	-3.54
7111	0.45	-3.65
7111	0.35	-3.78
7113	0.01	-3.68
7116	0.60	-7.89
7119	0.91	-7.18
7122	1.97	-7.41
7125	2.25	-7.25
7128	2.30	-7.77
7130	2.43	-7.31
7130	2.34	-7.49
7132	2.16	-7.23
7135	2.40	-4.35
7138	2.51	-7.32
7141	2.05	-7.64
7145	2.19	-6.99
7148	2.44	-7.03
7151	2.26	-7.43
7154	2.40	-7.14
7157	2.05	-7.69
7160	2.15	-7.44
7163	1.76	-7.82
7166	1.65	-7.64
7169	1.11	-7.52
7172	1.58	-7.30
7175	1.62	-7.05
7178	1.04	-6.91
7181	0.87	-8.28
7182	0.90	-8.15
7184	0.62	-8.04
7187	1.30	-6.99
7189	0.79	-7.26
7190	0.68	-7.77

7193	0.87	-7.06
7196	1.07	-7.55
7199	1.34	-7.79
7200	1.50	-6.48
7202	1.33	-7.22
7205	1.16	-7.54
7208	1.65	-6.93
7209	1.30	-6.51
7211	1.40	-7.34
7214	1.37	-8.35
7217	1.97	-8.35
7220	2.13	-8.01
7223	2.05	-6.89
7226	1.92	-5.54
7229	1.68	-7.12
7232	0.88	-8.04
7235	0.80	-8.01
7236	0.58	-7.60
7245	0.82	-8.11
7248	0.31	-7.36
7251	0.71	-6.35
7254	0.67	-6.62
7257	0.62	-6.29
7257	0.54	-6.33
7260	0.86	-5.98
7260	0.77	-6.04
7262	1.10	-5.73
7262	1.05	-5.61
7264	1.27	-4.20
7264	1.15	-4.29
7266	1.20	-4.15
6963	2.98	-7.91
6966	2.37	-6.39
6969	2.50	-6.08
6972	1.26	-7.75
6981	0.64	-6.65
6984	1.30	-5.56
6987	0.60	-5.59
6990	0.53	-5.51
6993	0.54	-6.06
6996	0.12	-5.79
6999	0.12	-5.31

7002	-0.10	-6.00
7004	-0.27	-5.60
7007.75	-0.23	-5.91
7011	-0.15	-6.29
7014	-0.14	-4.88
7017	3.75	-7.60
7020	3.38	-7.47
7023	2.01	-7.25
7026	3.38	-7.42
7029	3.71	-7.65
7032	4.26	-7.49
7035	4.59	-7.89
7038	4.99	-7.41
7041	5.07	-7.66
7044	4.94	-7.12
7047	4.56	-7.09
7050	3.45	-7.54
7053	1.85	-6.72
7056	1.25	-6.97
7059	0.56	-7.15
7062	0.79	-5.97
7065	0.56	-6.74
7068	0.26	-6.75
7071	0.70	-6.88
7074	0.34	-7.02
7077	0.42	-5.84
7080	0.96	-6.57
7083	1.02	-6.36
7086	1.24	-6.01
7089	0.40	-7.14
7092	0.40	-6.75
7095	0.89	-5.37
7098	1.03	-5.29
7101	0.99	-6.00
7104	0.76	-5.38
7107	0.62	-5.41
7110	0.54	-3.54
7111	0.45	-3.65
7111	0.35	-3.78
7113	0.01	-3.68
7116	0.60	-7.89
7119	0.91	-7.18

7122	1.97	-7.41
7125	2.25	-7.25
7128	2.30	-7.77
7130	2.43	-7.31
7130	2.34	-7.49
7132	2.16	-7.23
7135	2.40	-4.35
7138	2.51	-7.32
7141	2.05	-7.64
7145	2.19	-6.99
7148	2.44	-7.03
7151	2.26	-7.43
7154	2.40	-7.14
7157	2.05	-7.69
7160	2.15	-7.44
7163	1.76	-7.82
7166	1.65	-7.64
7169	1.11	-7.52
7172	1.58	-7.30
7175	1.62	-7.05
7178	1.04	-6.91
7181	0.87	-8.28
7182	0.90	-8.15
7184	0.62	-8.04
7187	1.30	-6.99
7189	0.79	-7.26
7190	0.68	-7.77
7193	0.87	-7.06
7196	1.07	-7.55
7199	1.34	-7.79
7200	1.50	-6.48
7202	1.33	-7.22
7205	1.16	-7.54
7208	1.65	-6.93
7209	1.30	-6.51
7211	1.40	-7.34
7214	1.37	-8.35
7217	1.97	-8.35
7220	2.13	-8.01
7223	2.05	-6.89
7226	1.92	-5.54
7229	1.68	-7.12

7232	0.88	-8.04
7235	0.80	-8.01
7236	0.58	-7.60
7245	0.82	-8.11
7248	0.31	-7.36
7251	0.71	-6.35
7254	0.67	-6.62
7257	0.62	-6.29
7257	0.54	-6.33
7260	0.86	-5.98
7260	0.77	-6.04
7262	1.10	-5.73
7262	1.05	-5.61
7264	1.27	-4.20
7264	1.15	-4.29
7266	1.20	-4.15
Johnson #1-6		
8193.00	2.10	-5.90
8192.00	1.90	-6.37
8191.00	1.79	-5.90
8190.00	2.20	-6.20
8189.00	1.62	-6.18
8188.00	1.76	-6.03
8187.00	1.58	-6.49
8186.00	1.48	-6.72
8185.00	1.59	-6.38
8184.00	1.84	-5.93
8183.00	1.38	-6.43
8182.00	1.59	-6.66
8181.00	1.62	-6.76
8180.00	1.58	-6.58
8179.00	1.87	-6.85
8178.00	1.63	-6.79
8177.00	1.42	-7.13
8176.00	1.33	-7.49
8175.00	2.09	-6.48
8174.00	1.28	-7.13
8174.00	1.35	-7.13
8174.00	1.35	-7.23
8173.00	1.96	-6.53
8172.00	1.77	-6.46
8171.00	1.35	-6.45

8170.00	1.42	-7.07
8169.00	1.39	-6.40
8168.00	1.38	-6.99
8167.00	1.43	-6.07
8166.00	1.59	-7.13
8165.00	1.41	-6.03
8164.00	1.74	-6.77
8163.00	1.51	-7.21
8162.00	1.22	-7.03
8161.00	1.63	-6.94
8160.00	2.08	-5.75
8159.00	1.88	-6.65
8158.00	2.01	-6.00
8157.00	1.60	-6.98
8157.00	1.67	-6.87
8157.00	1.66	-6.86
8156.00	1.60	-6.08
8156.00	1.64	-6.19
8156.00	1.62	-6.15
8155.00	2.26	-6.09
8154.00	1.07	-6.89
8153.00	1.50	-6.69
8152.00	1.27	-6.87
8151.00	1.20	-6.58
8150.00	1.38	-6.46
8149.00	1.33	-6.05
8148.00	1.14	-6.86
8147.00	1.30	-5.03
8146.00	0.88	-7.25
8145.00	1.13	-6.71
8144.00	1.60	-6.30
8143.00	1.56	-6.03
8142.00	1.70	-6.49
8141.30	1.15	-5.95
8140.00	1.36	-7.01
8139.00	1.04	-6.86
8138.00	0.53	-6.63
8137.00	1.33	-6.39
8136.00	1.58	-6.59
8135.00	1.31	-6.32
8134.00	1.21	-5.90
8133.00	0.79	-5.64

8132.00	0.95	-6.29
8131.00	1.30	-5.27
8130.00	1.29	-5.70
8129.00	1.11	-6.02
8128.00	1.29	-5.23
8127.00	1.36	-5.29
8126.00	1.20	-5.70
8125.00	1.23	-5.44
8124.00	1.00	-4.94
8123.00	0.81	-6.17
8122.00	1.00	-6.19
8121.00	0.93	-6.13
8120.00	1.01	-6.05
8119.00	1.29	-5.37
8118.00	1.18	-5.52
8117.00	1.04	-5.34
8116.00	0.92	-5.44
8115.00	1.18	-5.59
8114.00	1.42	-5.21
8113.00	1.50	-5.99
8112.00	2.23	-5.52
8111.00	2.95	-5.10
8110.00	3.00	-5.24
8109.00	2.40	-4.76
8108.00	1.19	-5.45
8107.00	0.99	-5.62
8107.00	1.01	-5.58
8107.00	0.97	-5.50
8106.00	0.97	-5.11
8106.00	1.08	-4.95
8106.00	1.07	-4.85
8105.00	1.10	-5.79
8104.00	1.10	-5.86
8103.50	1.29	-5.58
Snowplow #1-5		
5746.00	1.26	-4.99
5743.00	1.18	-4.68
5740.00	1.46	-3.63
5737.00	1.62	-4.97
5734.00	0.79	-5.74
5731.00	0.79	-6.29
5728.00	0.85	-6.09

5725.00	1.13	-5.48
5722.00	1.05	-6.21
5719.00	1.05	-5.79
5716.00	1.10	-6.24
5713.00	1.07	-5.89
5709.75	0.61	-6.05
5707.00	1.42	-6.27
5704.00	1.52	-6.01
5701.00	1.37	-6.02
5698.00	1.38	-5.97
5695.00	1.30	-6.17
5692.00	1.36	-5.99
5689.00	0.96	-6.09
5686.00	0.53	-6.25
5683.00	1.43	-4.89
5680.00	1.81	-4.15
5677.00	1.26	-3.38
5674.00	0.95	-4.78
5671.00	1.53	-3.76
5668.00	2.02	-4.94
5665.00	1.85	-5.07
5662.00	1.74	-4.19
5659.00	0.88	-5.85
5656.00	2.05	-2.81
5653.00	1.92	-2.80
5650.25	1.30	-4.42
5644.85	1.09	-6.30
5641.00	1.44	-6.02
5638.00	1.42	-7.09
5636.40	1.98	-4.36
5633.00	1.85	-4.05
5632.00	1.79	-3.93
5624.00	1.06	-5.44
5621.00	0.96	-5.62
5618.00	0.83	-5.53
5615.00	1.80	-6.51
5612.00	1.20	-5.81
5609.00	1.10	-5.63
5606.00	1.26	-6.02
5597.00	0.87	-6.04
5594.00	0.92	-6.27
5591.00	1.87	-5.34

5588.00	1.87	-5.01
5585.00	1.72	-5.75
5582.00	1.06	-5.45
5579.00	1.22	-5.69
5576.00	1.12	-5.89
5573.50	1.51	-5.27
Snowplow #4-6		
5589.00	1.51	-5.45
5586.00	1.80	-5.61
5583.00	3.07	-5.62
5580.00	4.02	-4.81
5577.00	3.59	-5.47
5574.00	3.76	-5.47
5571.00	3.47	-5.71
5568.00	3.30	-5.10
5565.00	4.12	-5.31
5562.00	3.20	-5.19
5559.00	3.02	-5.35
5556.00	2.57	-4.85
5553.00	1.96	-5.43
5550.00	-0.45	-5.51
5548.00	-0.70	-5.81
5546.00	-0.53	-4.87
5543.00	0.42	-4.89
5540.00	0.44	-5.37
5537.00	0.40	-5.86
5534.00	-0.27	-5.32
5530.00	1.01	-5.22